RESEARCH ARTICLE

Biofactors WILEY

ErbB2-NOTCH1 axis controls autophagy in cardiac cells

Francesca Fortini[1] | Francesco Vieceli Dalla Sega[1] | Edoardo Lazzarini[2,3] | Giorgio Aquila[4] | Polina Sysa-Shah[5] | Edoardo Bertero[6] | Alessia Ascierto[4] | Paolo Severi[4] | Achille Wilfred Ouambo Talla[4] | Alessio Schirone[7] | Kathleen Gabrielson[8,9,10] | Giampaolo Morciano[1,11] | Simone Patergnani[11] | Gaia Pedriali[1] | Paolo Pinton[1,11] | Roberto Ferrari[4] | Elena Tremoli[1] | Pietro Ameri[6,12] | Paola Rizzo[1,4]

[1]GVM Care & Research, Maria Cecilia Hospital, Ravenna, Italy

[2]Laboratory for Cardiovascular Theranostics, Cardiocentro Ticino Institute, Ente Ospedaliero Cantonale Lugano, Lugano, Switzerland

[3]Euler Institute, Faculty of Biomedical Sciences, Università della Svizzera italiana, Lugano, Switzerland

[4]Department of Translational Medicine and Laboratory for Technologies of Advanced Therapies (LTTA), University of Ferrara, Ferrara, Italy

[5]The Brady Urological Institute and Department of Urology, Johns Hopkins University, School of Medicine, Baltimore, Maryland, USA

[6]Department of Internal Medicine and Specialties (Di.M.I.), University of Genova, Genova, Italy

[7]Oncology and Hematology Department, Azienda Ospedaliero-Universitaria di Ferrara, Ferrara, Italy

[8]Department of Molecular and Comparative Pathobiology, Johns Hopkins University School of Medicine, Baltimore, Maryland, USA

[9]Department of Pathology, Johns Hopkins University School of Medicine, Baltimore, Maryland, USA

[10]Sidney Kimmel Comprehensive Cancer Center, Johns Hopkins University, Baltimore, Maryland, USA

[11]Department of Medical Sciences, University of Ferrara, Ferrara, Italy

[12]Cardiac, Thoracic, and Vascular Department, IRCCS Ospedale Policlinico San Martino, Genoa, Italy

Correspondence
Francesca Fortini and Paola Rizzo, Maria Cecilia Hospital, GVM Care & Research, Cotignola, Ravenna, Italy.
Email: ffortini@gvmnet.it; rzzpla@unife.it

Abstract

Although the epidermal growth factor receptor 2 (ErbB2) and Notch1 signaling pathways have both significant roles in regulating cardiac biology, their interplay in the heart remains poorly investigated. Here, we present evidence of a crosstalk between ErbB2 and Notch1 in cardiac cells, with effects on autophagy and proliferation. Overexpression of ErbB2 in H9c2 cardiomyoblasts induced Notch1 activation in a post-transcriptional, p38-dependent manner, while ErbB2 inhibition with the specific inhibitor, lapatinib, reduced Notch1 activation. Moreover, incubation of H9c2 cells with lapatinib resulted in stalled autophagic flux and decreased proliferation, consistent with the established cardiotoxicity of this and other ErbB2-targeting drugs. Confirming the findings in H9c2 cells, exposure of primary neonatal mouse cardiomyocytes to exogenous neuregulin-1, which engages ErbB2, stimulated proliferation, and this effect was abrogated by concomitant inhibition of the enzyme responsible for Notch1 activation. Furthermore, the hearts of transgenic mice specifically

Francesca Fortini, Francesco Vieceli Dalla Sega, and Edoardo Lazzarini have contributed equally to this work and share first authorship.

Pietro Ameri and Paola Rizzo share senior authorship.

overexpressing ErbB2 in cardiomyocytes had increased levels of active Notch1 and of Notch-related genes. These data expand the knowledge of ErbB2 and Notch1 functions in the heart and may allow better understanding the mechanisms of the cardiotoxicity of ErbB2-targeting cancer treatments.

KEYWORDS

autophagy, cardiomyocytes, ErbB2, heart, Notch

1 | INTRODUCTION

ErbB2 (also known as HER2, human epidermal growth factor receptor 2) is a member of the epidermal growth factor receptor (EGFR) family with major roles in cardiac development, preservation of homeostasis, and response to stress.[1] In the postnatal heart, the action of ErbB2 is mostly related to the formation of heterodimers with another EGFR, ErbB4, following binding of the latter by neuregulin-1 (NRG-1), with ensuing initiation of protective signaling pathways.[2]

Numerous studies have shown that ErbB2 inhibition impairs the function and survival of cardiomyocytes by affecting mitochondrial function[3,4] and metabolism,[5] promoting apoptosis.[6,7] ErbB2 inhibition in cardiomyocytes causes increased oxidative stress,[4,8] while its overexpression upregulates antioxidant enzymes and reduces basal levels of reactive oxygen species (ROS), protecting against doxorubicin-induced cardiotoxicity.[9] It has also been suggested that disruption of ErbB2-driven signaling leads to dysregulated autophagy, which is particularly crucial for maintaining tissue homeostasis in post-mitotic cells, such as cardiomyocytes, by recycling cellular components and damaged organelles.[10,11] Based on this evidence, defective ErbB2 activity has been implicated in cardiac disease.

The importance of ErbB2 in cardiac biology—and of ErbB2 blockade in cardiac pathology—was discovered after finding an unexpectedly high rate of left ventricular dysfunction and heart failure (HF) in pivotal clinical trials testing trastuzumab, a monoclonal antibody against HER2, in patients with breast cancer. Approximately 20% of human breast cancers overexpress HER2, which is constitutively activated and promotes cell cycle progression and proliferation in a ligand-independent manner.[12] Hence, HER2-expressing breast cancer is more aggressive and confers a poorer prognosis than HER2-negative breast cancer.[13] Consequently, trastuzumab and more recent HER2-targeting drugs, including pertuzumab, another monoclonal antibody, and lapatinib, a tyrosine kinase inhibitor (TKI), improve outcomes in patients with HER2-positive breast cancer. However, off-target blockade of HER2 in the heart may cause cardiotoxicity.[14]

It is notable that the negative effects of therapies against HER2 cannot be solely explained by interference with the NRG-1/HER2-HER4 axis. According to their pharmacokinetics, trastuzumab, pertuzumab, and lapatinib are predicted to variably affect the heterodimerization of HER2 with HER4 and may even act irrespective of ligand occupancy of the receptor.[15] Furthermore, trastuzumab elicits modifications in human pluripotent stem cell-derived cardiomyocytes in the absence of exogenous NRG-1.[16]

In breast cancer cells, ErbB2 inhibition modulates Notch1 signaling.[17,18] Notch1 is one of four receptors (Notch1, 2, 3, and 4) located on the plasma membrane and activated in a juxtacrine manner by five ligands present on the surface of adjacent cells, namely Delta-like (Dll)-1, −3, and −4, and Jagged-1 and -2. In the so-called canonical pathway, the binding of a ligand triggers two proteolytic cleavages of the Notch receptor, the second being mediated by γ-secretase. This results in the release of the active form of Notch (Notch intracellular domain, NICD), which translocates into the nucleus and regulates the transcription of several genes, including the *HES* (Hairy and Enhancer of Split) and *HEY* (Hairy and Enhancer of Split with YRPW) genes family. In the non-canonical pathway, Notch is activated even in the absence of established ligands or NICD activates/inhibits cytoplasmic proteins.[19]

The Notch pathway is crucial for heart development. It is turned off in adult cardiomyocytes, but can be reactivated following injury to induce survival, proliferative, and regenerative signaling[20] by regulating mitochondrial function,[21] reducing oxidative stress,[22] controlling the proliferation and differentiation of cardiomyocytes,[23,24] preventing cardiomyocyte apoptosis,[25–27] and reducing fibrosis.[28]

Unlike in breast cancer, the crosstalk between ErbB2 and Notch1 has not been investigated in cardiac cells. We sought to bridge this gap in knowledge by investigating whether Notch1 is modulated by ErbB2 in H9c2 cardiomyoblasts and cardiomyocytes and elucidating the potential cellular functions regulated by the ErbB2/Notch1 axis.

2 | EXPERIMENTAL PROCEDURES

2.1 | Materials

Antibodies used were: goat polyclonal to Notch1 (C-20, catalog number sc-6014), which recognizes the C-terminus of the protein, identifying all forms of Notch1, from Santa Cruz Biotechnology (Santa Cruz, CA, USA); rabbit polyclonal to caspase-3 (catalog number #9662), rabbit monoclonal to cleaved Notch1 valine 1744 (an antibody directed against valine-1744 at the N-terminus of the cleaved form of Notch1, catalog number #4147), rabbit monoclonal to phospho-p38 MAPK (Thr180/Tyr182) (D3F9) (catalog number #9211), rabbit polyclonal to p38 MAPK (catalog number #9212) rabbit polyclonal to phospho-Akt (Ser473 catalog number #9271), rabbit polyclonal to Akt (catalog number #9272), rabbit monoclonal to phospho-p44/42 MAPK (Erk1/2) (Thr202/Tyr204) (D13.14.4E) (catalog number #4370), rabbit monoclonal to p44/42 MAPK (Erk1/2) (137F5) (catalog number #4695), rabbit monoclonal to phospho-SAPK/JNK (Thr183/Tyr185) (98F2) (catalog number #4668), rabbit monoclonal to SAPK/JNK (catalog number #9252) from Cell Signaling Technology (Beverly, MA, USA); rabbit monoclonal antibody to Bax (catalog number ab32503), rabbit polyclonal antibody to Bcl-2 (catalog number ab196495) and rabbit monoclonal antibody to Ki67 (catalog number ab16667) from Abcam (Cambridge, UK); mouse monoclonal antibody to β-actin (AC-15, catalog number A5441), rabbit polyclonal antibody to p62/SQSTM1 (catalog number P0067) and rabbit polyclonal antibody to LC3 B (catalog number L8918) from Sigma Aldrich (St. Louis, MO, USA). Dulbecco's modified Eagle's medium (DMEM) was from Euroclone (Milan, Italy). Fetal bovine serum (FBS), DAPI ProLong, Lipofectamine LTX, Opti-MEM reduced-serum medium, Annexin V-FITC, propidium iodide (PI), mitoSOX, SuperScript III reverse transcriptase, random hexamers, dNTPs, primers for RT-PCR, RNaseOut, and RNAse A were from ThermoFisher Scientific (Waltham, MA, USA). Trans-Blot® Turbo™ Mini Nitrocellulose Transfer Packs, Clarity™ Western ECL Substrate, Precast Protein Gels, 10x Tris/Glycine/SDS were from BioRad (Hercules, CA, USA). RNeasy Mini Kit was from Qiagen (Hilden, Germany). PerfeCta SYBR Green SuperMix with ROX kit was from Quanta Biosciences (Gaithersburg, MD). β-Galactosidase staining kit was purchased from Cell Signaling Technology (Beverly, MA, USA). MK-0752 and SP600125 were purchased from MedChemExpress (Monmouth Junction, NJ, USA). Lapatinib, γ-secretase inhibitor DAPT, SB203580, tetramethylrhodamine methyl ester (TMRM), carbonyl cyanide p-trifluoromethoxyphenylhydrazone (FCCP), and other materials were purchased from Sigma Aldrich (St. Louis, MO, USA).

2.2 | Methods

2.2.1 | Cell culture

H9c2 rat cardiomyoblasts were purchased from American Type Culture Collection (ATCC, Manassas, VA). Cells were cultured in DMEM supplemented with 10% FBS and incubated at 37°C in a 5% CO_2 atmosphere. 1% penicillin/streptomycin was added in the medium. H9c2 were seeded at a density of $1 \times 10^4/cm^2$ and used for experiments when they were 70%–80% confluent.

2.2.2 | Transfection with plasmids

H9c2 cells were transfected with 0.5 μg/mL of pcDNA3 vector encoding Notch1ICD (N1ICD, a gift from Dr. Lucio Miele, LSU Health Sciences Center School of Medicine, New Orleans, Louisiana), 1 μg/mL of pcDNA3 vector encoding ErbB2 or the empty vector as control (pcDNA3 CTRL), using Lipofectamine LTX (ThermoFisher Scientific). Cell treatment with lapatinib 5 μM or SB203580 10 μM began 18 h after transfection. The concentration of lapatinib used for treatments was determined based on published studies in H9c2 cells[29] and clinical studies.[30]

2.2.3 | Proliferation assay

H9c2 cells were stained with Trypan blue 24, 48, and 72 h after adding lapatinib 5 μM and were counted in a Burker chamber.

2.2.4 | Apoptosis

Apoptosis was assessed with the Annexin V-FITC binding assay as previously described.[31] Briefly, H9c2 cells were grown in the presence of treatment, then collected and stained with Annexin V-FITC (ThermoFisher Scientific) (100 ng/mL) and propidium iodide (PI) (ThermoFisher Scientific) (10 μg/mL). Flow cytometric analysis and data analysis were performed with Attune Nxt Flow cytometer and Attune Nxt Software (ThermoFisher Scientific), respectively. Apoptosis levels were expressed as percentages of Annexin V-positive cells out of the total number of cells. As a technical positive control, we treated H9c2 with 1 μM staurosporine for 6 h.

2.2.5 | β-Galactosidase staining

Senescence-associated β-galactosidase (SA-β-gal) activity was determined using a Senescence β-Galactosidase staining kit (Cell Signaling), following the manufacturer's protocols. Briefly, H9c2 cells were fixed for 15 min at room temperature and then treated with β-Galactosidase Staining Solution and incubated at 37°C overnight in a dry incubator without CO_2. Senescence was quantified by visually inspecting blue-stained cells under a microscope (Nikon Eclipse Ts2) using 10X objectives. Results were expressed as the mean of blue-stained cells counted in five visual fields of three independent experiments. As a technical positive control, we treated human umbilical vein endothelial cells (HUVECs), cultured as previously described,[32] with 0.1 μM of doxorubicin for 72 h.

2.2.6 | Immunofluorescence

For immunofluorescence analysis, H9c2 cells were fixed in 4% PFA. Cells were permeabilized, blocked, and then incubated overnight at 4°C with rabbit anti-Ki67. Following three washes, the cells were incubated for 1 h at room temperature in the dark with anti-rabbit antibody conjugated with Alexa Fluor 633 (ThermoFisher Scientific) and then mounted with DAPI ProLong. The images were acquired using a confocal microscope (Nikon A1 System) using 20X objectives. Ki67 positive cells were counted using ImageJ software. Results were expressed as percentage of Ki67-positive cells in 5 visual fields of three independent experiments.

2.2.7 | Western blot

Western blot was performed as previously described.[32] Briefly, cells were lysed on ice for 30 min in RIPA Lysis and Extraction buffer (ThermoFisher Scientific). Heart tissue was harvested and homogenized with TissueLyser (Qiagen), 20 mg of tissue was shaken at 120 Hz for two repetitions of 2 min in the same buffer then left on ice for 30 min. Equal amounts of total proteins were separated on Mini-PROTEAN® TGX™ (Biorad) and transferred into nitrocellulose membranes using the Trans-Blot® Turbo system (Biorad). After the blocking step, the membranes were incubated overnight at 4°C with the primary antibodies and then with secondary peroxidase-conjugated antibodies. For immunodetection, membranes were incubated with Clarity™ or Clarity™ Max Western ECL blotting substrates (Biorad), and the images were obtained with ChemiDoc camera (Biorad).

2.2.8 | Reverse transcription (RT) – PCR

RNA was extracted using the RNeasy Mini Kit (Qiagen) and quantified with Nanodrop (ThermoFisher Scientific). RT-PCR was performed as previously described.[33] Briefly, 500 ng of RNA were reverse transcribed using Super-Script™ First-Strand Synthesis System (ThermoFisher Scientific). The Real-time PCR experiments were conducted on the StepOne™ Real-Time PCR System using Perfecta SYBR Green SuperMix with ROX kit (Quanta Biosciences). The final concentration of all the primers was 500 nM. Primer sequences: *Rpl13a*: forward 5′-CCGCAAGATCCGCAGACGCA-3′, reverse 5′-CTGA-TGGGACCGGACGCGG-3′; *Notch1*: forward 5′-GGT-GCGAGCGCAGTGAAGGA-3′, reverse 5′-CCCGCTGCT GCCCTCTTTCC-3′; *Hey1*: forward 5′-TCGTCCCAGG-TTTTGGCCCG-3′, reverse 5′-TCTAGCTTCGCAGATCC-CTGCT-3′; *Hey2*: forward 5′-TTTCGCCGCGATGA AGCGCC-3′, reverse 5′-TGAGCTTGCACTGTGCCCG-GAG-3′; *Hes1*: forward 5′-ATTCCTCGTCCCCGG-TGGCT-3′, reverse 5′-TCTTGCCCGGCGCCTCTTCT-3′. Changes in gene expression were calculated by the $2^{-\Delta\Delta Ct}$ formula using *Rpl13a* as the reference gene.

2.2.9 | GFP-LC3 fluorescence

Autophagy was assessed by using green fluorescent protein (GFP)-tagged microtubule-associated protein light chain 3 (LC3) expressing cells. GFP-LC3 expression plasmid (0.8 μg) with plasmid encoding Notch1 (1.2 μg) or empty (pcDNA3 CTRL) were transfected using Lipofecta-mine LTX (ThermoFisher Scientific). H9c2 cells were treated with lapatinib 5 μM for 24 h and then fixed with PFA 4% for 15 min. Fluorescence analysis was carried out on a confocal microscope (Nikon A1 System) using 60X objectives. Results were expressed as mean of the number of GFP-LC3 dots per cell counted in three visual fields of three independent experiments.

2.2.10 | Cell cycle analysis

For cell cycle analysis, H9c2 were fixed in pre-cooled 70% ethanol for 30 min on ice, and subsequently washed with PBS 1X before being centrifuged. The resulting cell pellet was then resuspended in a PI staining solution consisting of 0.1% Triton X-100, 50 μg/mL PI, and 100 μg/mL RNAse A in PBS 1X, and incubated for 30 min at room temperature. Finally, PI fluorescence was measured using Attune Nxt Flow cytometer (ThermoFisher Scientific), and the data were analyzed with Attune Nxt Software (ThermoFisher Scientific).

2.2.11 | Basal mitochondrial membrane potential

Cells were loaded with 20 nM tetramethylrhodamine methyl ester (TMRM) for 30 min at 37°C. To obtain and analyze basal levels, cells were stimulated with 10 nM carbonyl cyanide p-trifluoromethoxyphenylhydrazone (FCCP), a strong uncoupler of oxidative phosphorylation. Image acquisitions were performed with a motorized Nikon AX R confocal microscope with a 40X/0.6 PlanApo objective and laser LU-N4S 405/488/561/640.

2.2.12 | Mitochondrial ROS measurements

ROS measurements were performed according to the procedure proposed by the authors in reference 34. Briefly, measurements of mitochondrial superoxide ($mtO_2^{\bullet-}$) production were performed on cells incubated for 30 min at 37°C in the presence of 5 μM mitoSOX red. The fluorescence was evaluated on Nikon AX R confocal microscope with a PlanApo 60X/1.4 objective and laser LU-N4S 405/488/561/640.

2.2.13 | Primary neonatal mouse cardiomyocytes

Neonatal cardiac cells were harvested from 1 to 2 days-old C57BL/6 pups (IRCCS Ospedale Policlinico San Martino approval 792/2015-PR) and cultured with or without NRG-1100 ng/mL and/or γ-secretase inhibitor MK-0752 (MK) 5 μM. Experiments were started 24 h after seeding cells and cardiomyocyte proliferation was examined by counting cells co-stained for troponin T and Ki67.

2.2.14 | ErbB2 transgenic mice

The study was performed in accordance with the Guide for the Care and Use of Laboratory Animals of the National Institutes of Health recommendations. The protocol was approved by the Animal Care and Use Committee of the Johns Hopkins Medical Institutions (Animal Welfare Assurance No. A-3273-01). The wild-type (WT) and transgenic (TG; ErbB2^{tg}) mice used in this study were developed as described previously.[35] All the wild-type and transgenic mice were housed under a 12 h light–dark cycle with free access to food and water. Expression of Notch1 and N1ICD was assessed in total heart lysates from 1-week-old and 2-week-old male animals.

2.2.15 | mRNA microarray

Total RNA was isolated from the hearts of 3 months-old wild type and ErbB2^{tg} male mice (4 animals per group). Agilent G4122A mouse 44 K microarray slides were used to analyze gene expression in cardiac tissue. These genes were analyzed by cluster analysis to delineate patterns of expression between the two groups. Differentially expressed genes (DEGs) were identified by $\log_2$ z-transformation followed by the significance analysis of microarray consisting of: statistical significance (z-test p-value ≤0.05) and absolute z ratio threshold (|z ratio| ≤ 1.5); probe average z score signal for each pairwise comparisons ≥0; a sample group level one-way ANOVA p-value ≤0.05 globally for sample group character quality; and probe detect p-value ≤0.01 to ensure good quality signal. The same gene may appear more than once if different probes have been used for a single gene. Genes were assigned to Gene Ontology gene sets (MSigDB).

2.2.16 | Statistical analyses

Results are expressed as mean ± SEM of at least three independent experiments. For comparisons between two groups, two-tailed unpaired Student's t test was used. When more than two groups were compared, one-way analysis of variance and multiple comparisons test were used.

3 | RESULTS

3.1 | ErbB2 is upstream of Notch1 activation in H9c2 cells

To investigate the possible regulation of Notch1 by ErbB2 in cardiomyocytes, we overexpressed ErbB2 by transfecting H9c2 cells with a plasmid containing the sequence of rat *ErbB2*. Overexpression of ErbB2 was confirmed by Western blot (Figure 1A). H9c2 cells transfected with ErbB2 showed an increase of Notch1 intracellular domain (N1ICD), the active form of Notch1, compared to cells transfected with the empty vector (pcDNA3) (Figure 1A). ErbB2 overexpression did not affect *Notch1* mRNA levels, suggesting that the effect of ErbB2 on Notch1 is post-transcriptional (Figure 1B). Conversely, we observed an increase in *Hey2* (Hairy and Enhancer of Split with YRPW-2) expression and, although not statistically significant, a trend for an increase in the expression of the other Notch target genes *Hey1* and *Hes1* (Hairy and Enhancer of Split-1) (Figure 1B). Since p38 activation

increases N1ICD in RAS-transformed human cells,[36] we investigated the possible role of p38 MAPK also in ErbB2-mediated Notch1 activation. First, we estimated the activation of p38, and found an increase in p38 phosphorylation in cells overexpressing ErbB2 compared to the cells transfected with the empty vector (Figure 1A). To determine whether ErbB2 enhanced N1ICD formation through a p38-mediated mechanism, H9c2 cells were then treated for 24 h with 10 μM SB203580, a p38 MAPK inhibitor, and N1ICD protein level was determined by Western blot. Cells overexpressing ErbB2 showed an increase of N1ICD, which was reduced by SB203580 (Figure 1C). Additionally, to investigate whether other kinases are involved in ErbB2-mediated Notch1 activation, we evaluated the phosphorylation of AKT, p44/42 (also called ERK1/2) and SAPK/JNK in H9c2 overexpressing ErbB2 compared to cells transfected with the empty vector. ErbB2 overexpression determined an increase in SAPK/JNK phosphorylation, while the phosphorylation of AKT and ERK1/2 remained unchanged (Supplementary Figure S1A). To determine the role of JNK in ErbB2-mediated induction of N1ICD, H9c2 cells were treated for 24 h with 100 μM SP600125, a JNK inhibitor, and N1ICD protein levels were determined by Western blot. The treatment with SP600125 induced N1ICD regardless of overexpression of ErbB2 (Supplementary Figure S1B). Since SP600125 increases the phosphorylation of p38 MAPK,[37] we hypothesized that the induction of N1ICD by SP600125 could be determined by activation of p38. To investigate this possibility, H9c2 cells were co-treated with SP600125 and SB203580, and N1ICD protein levels were determined by Western blot. We found that the SP600125-mediated increase in N1ICD was reduced by SB203580, confirming the role of p38 MAPK in Notch1 activation (Supplementary Figure S1C). Taken together, these results suggest that ErbB2 induces Notch1 activation, at least in part, by a p38-dependent mechanism.

To gain further evidence that ErbB2 controls Notch1 activation in H9c2 cells, we used the opposite approach, i.e. we inhibited ErbB2 through incubation with lapatinib, a selective, reversible, ATP-competitive TKI that reduces ErbB2 phosphorylation.[38] It is known that H9c2 cells express NRG-1 and ErbB2,[39] thus having a NRG-1-ErbB2 autocrine/paracrine axis. Cells were treated with two different concentrations of lapatinib (0.5 and 5 μM) for 24 h, then we determined the effect of ErbB2 inhibition on Notch1 protein and transcript levels and Notch target genes expression. We found that treatment with lapatinib 0.5 μM and 5 μM for 24 h significantly reduced the protein levels of Notch1 precursor (N1PC), Notch1 transmembrane (N1TM), and Notch1 intracellular domain (N1ICD) (Figure 2A), as well as *Notch1* mRNA

abundance (Figure 2B). Lapatinib also dose-dependently reduced the expression of Notch target genes, *Hey1* and *Hey2*, while the levels of *Hes1*, were lower, as compared with control, only after incubation with 5 μM lapatinib (Figure 2B). We further investigated *Hes1* response by testing additional concentrations of lapatinib (1 and 2 μM). Supplementary Figure S2 shows a reduction in *Hes1* expression starting at 1 μM, indicating that, likely due to multiple pathways regulation,[40] higher drug concentration is needed to affect *Hes1* mRNA compared to *Hey1* and *Hey2*.

## 3.2 | ErbB2 and Notch1 control autophagic flux in H9c2 cells

Since inhibition of ErbB2 causes dysregulation of autophagy in cardiomyocytes[41] and Notch1 has also been shown to modulate autophagy, albeit in lymphocytes,[42] we determined the levels of LC3-II and p62 in H9c2 cells in which the ErbB2 or Notch1 pathway were pharmacologically inhibited. When autophagy is activated, a cytosolic, cleaved, form of LC3 (LC3-I) is conjugated to phosphatidylethanolamine to form LC3-II, which is associated with autophagic vesicles; furthermore, p62, a ubiquitin-binding scaffold protein, delivers autophagy substrates to autophagosomes for degradation.[43]

Treatment with lapatinib 0.5 and 5 μM increased the protein level of LC3-II compared with untreated cells in a dose-dependent manner (Figure 3A). In addition, we observed an accumulation of p62 protein in H9c2 cells treated with lapatinib 5 μM for 24 h (Figure 3A). To determine whether the increase in LC3-II by lapatinib was due to autophagosome formation or accumulation of autophagosomes, we used bafilomycin A1 (BafA1) to suppress autophagic flux.[44] H9c2 cells were treated with lapatinib 5 μM for 24 h in the presence or absence of 100 nM BafA1 during the last 4 h of the treatment with lapatinib. Both BafA1 and lapatinib 5 μM increased the level of LC3-II and p62, but BafA1 did not further increase protein levels of both LC3-II and p62 in lapatinib-treated cells, suggesting that treatment with lapatinib determined a suppression of autophagic flux (Figure 3B). To confirm that the effects of lapatinib on Notch1 and autophagy are due to inhibition of ErbB2, we treated H9c2 cells with CP-724714, a selective inhibitor of ErbB2 autophosphorylation. We found that, similar to lapatinib, treatment with CP-724714 at 5 μM and 10 μM for 24 h significantly reduced N1ICD and induced LC3-II and p62 protein levels in a dose-dependent manner (Supplementary Figure S3). To address the question of whether Notch1 regulates autophagy in H9c2 cells, we used DAPT, a γ-secretase inhibitor that blocks Notch1
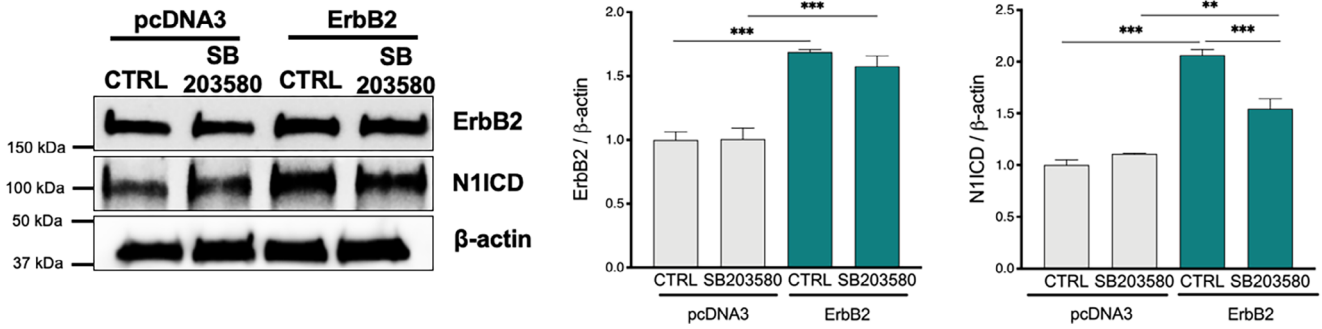
(A)
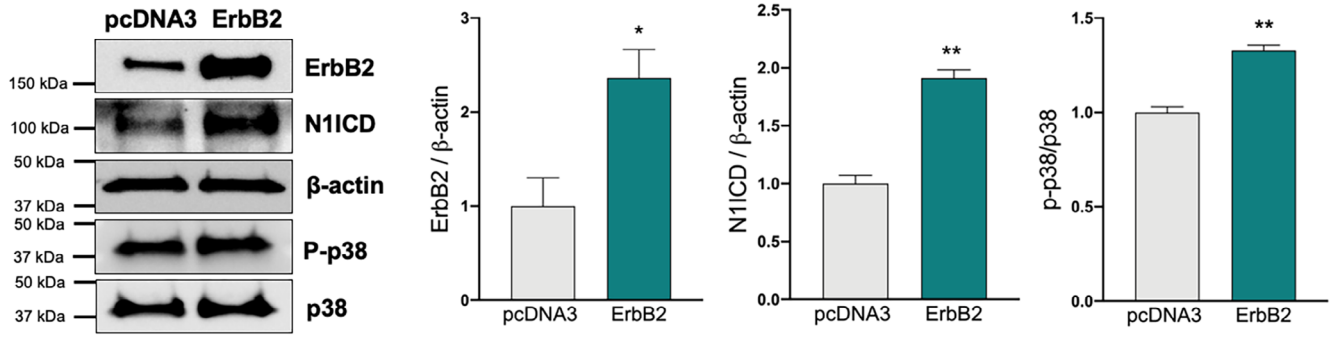
(B)
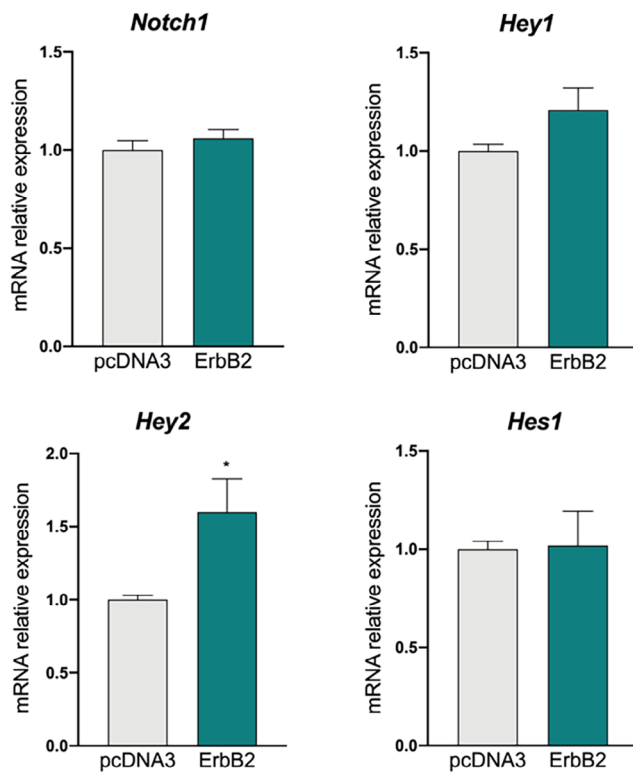
(C)

FIGURE 1   Legend on next page.

activation. After 24 h-incubation with 5 μM DAPT, N1ICD was significantly less than in control condition, as expected. Moreover, the levels of LC3-II and p62 protein were increased (Figure 3C). Similar to what we observed with lapatinib, we did not observe differences in LC3-II and p62 protein levels between H9c2 cells treated with DAPT alone or DAPT along with 100 nM BafA1 during the last 4 h of incubation, suggesting that inhibition of Notch1 activation led to autophagic flux blockade like inhibition of ErbB2 (Figure 3D).

3.3 | Notch1 overexpression rescues the autophagic flux impaired by lapatinib treatment in H9c2 cells

Building upon the evidence that ErbB2 is upstream of Notch1 and that both ErbB2 and Notch1 inhibition results in stalled autophagy in H9c2 cells, we hypothesized that forced activation of Notch1 would counteract the blockade of autophagic flux induced by lapatinib. To prove this, H9c2 cells were transfected with a plasmid containing the sequence of N1ICD or with an empty vector (pcDNA3), treated with lapatinib 5 μM, and evaluated for autophagy. Overexpression of N1ICD was confirmed by Western blot analysis (Figure 4A). Upon treatment with lapatinib 5 μM for 24 h, H9c2 cells overexpressing N1ICD showed reduced accumulation of LC3-II and p62 proteins, compared with cells transfected with the empty vector (Figure 4A). Autophagic flux was investigated also by using a plasmid expressing GFP-LC3.[45] H9c2 cells were transfected with a vector expressing GFP-LC3 in the presence or absence of the N1ICD-containing plasmid and then treated with lapatinib 5 μM for 24 h. Confocal microscopy images showed that lapatinib significantly increased the number of autophagosomes, represented by green puncta structures, compared to control untreated cells, and N1ICD overexpression counteracted this effect (Figure 4B). To assess the impact of autophagy blockade on mitochondria, we treated H9c2 cells with 5 μM lapatinib for 24 h and measured mitochondrial membrane potential (Δψm) and mitochondrial ROS (mtROS) levels. We observed an increase in both Δψm and mtROS, and N1ICD overexpression attenuated the increase in Δψm but not mtROS production (Supplementary Figure S4A,B). These results support the hypothesis that Notch1 is involved in ErbB2-driven stall of the autophagic flux in H9c2 cells.

3.4 | Block of autophagic flux by treatment with lapatinib is associated with proliferation, but not with apoptosis or senescence of H9c2 cells

To investigate the functional effects of lapatinib-induced block of autophagic flux, we assessed cell proliferation, apoptosis, and senescence. The number of H9c2 cells decreased after treatment with 5 μM lapatinib starting from 48 h of treatment (Figure 5A). Flow cytometric analysis did not reveal an increase in apoptosis in H9c2 cells treated with lapatinib 5 μM for 24, 48, and 72 h (Figure 5B). The proportion of senescent cells, under the experimental conditions used, was low and remained unchanged following up to 72-h exposure to lapatinib, as compared with control (Figure 5C). Thus, we concluded that the reduction in live cells upon prolonged treatment with lapatinib was secondary to inhibition of proliferation, rather than to apoptosis or senescence.

3.5 | Notch1 overexpression counteracts lapatinib-caused reduction of proliferation of H9c2 cells

To determine whether the overexpression of N1ICD, which restores the autophagic flux, could also reverse the

FIGURE 1 ErbB2 activates Notch1 through a p38-dependent mechanism. H9c2 cells were transfected with a plasmid containing the sequence for ErbB2 or with empty vector as control (pcDNA3) and the following analyses were performed: (A) (left) Western blotting analysis of the levels of ErbB2, Notch1 intracellular domain (N1ICD), p-p38 and p38 proteins. β-Actin was used as loading control; (right) Densitometric analysis of Western blots showing protein levels after the treatments normalized to untreated control levels, after signal comparison to β-Actin. Results are expressed as mean ± SEM of three independent experiments *p < 0.05; ** p < 0.01. (B) qRT-PCR analyses were performed to detect *Notch1*, *Hey1*, *Hey2*, and *Hes1* mRNA levels in H9c2 cells overexpressing ErbB2. Relative changes in mRNA expression levels were calculated according to the $2^{-\Delta\Delta Ct}$ method using *Rpl13A* as reference gene. Results are expressed as mean ± SEM of three independent experiments. *p < 0.05. (C) (left) Western blotting analysis of the levels of ErbB2 and N1ICD in H9c2 cells transfected with ErbB2 in the presence or absence of a p38 MAPK inhibitor, SB203580 10 μM, for 24 h. β-Actin was used as loading control; (right) Densitometric analysis of Western blots showing protein levels after the treatments normalized to untreated control levels, after signal comparison to β-Actin. Results are expressed as mean ± SEM of three independent experiments. ** p < 0.01; *** p < 0.001.
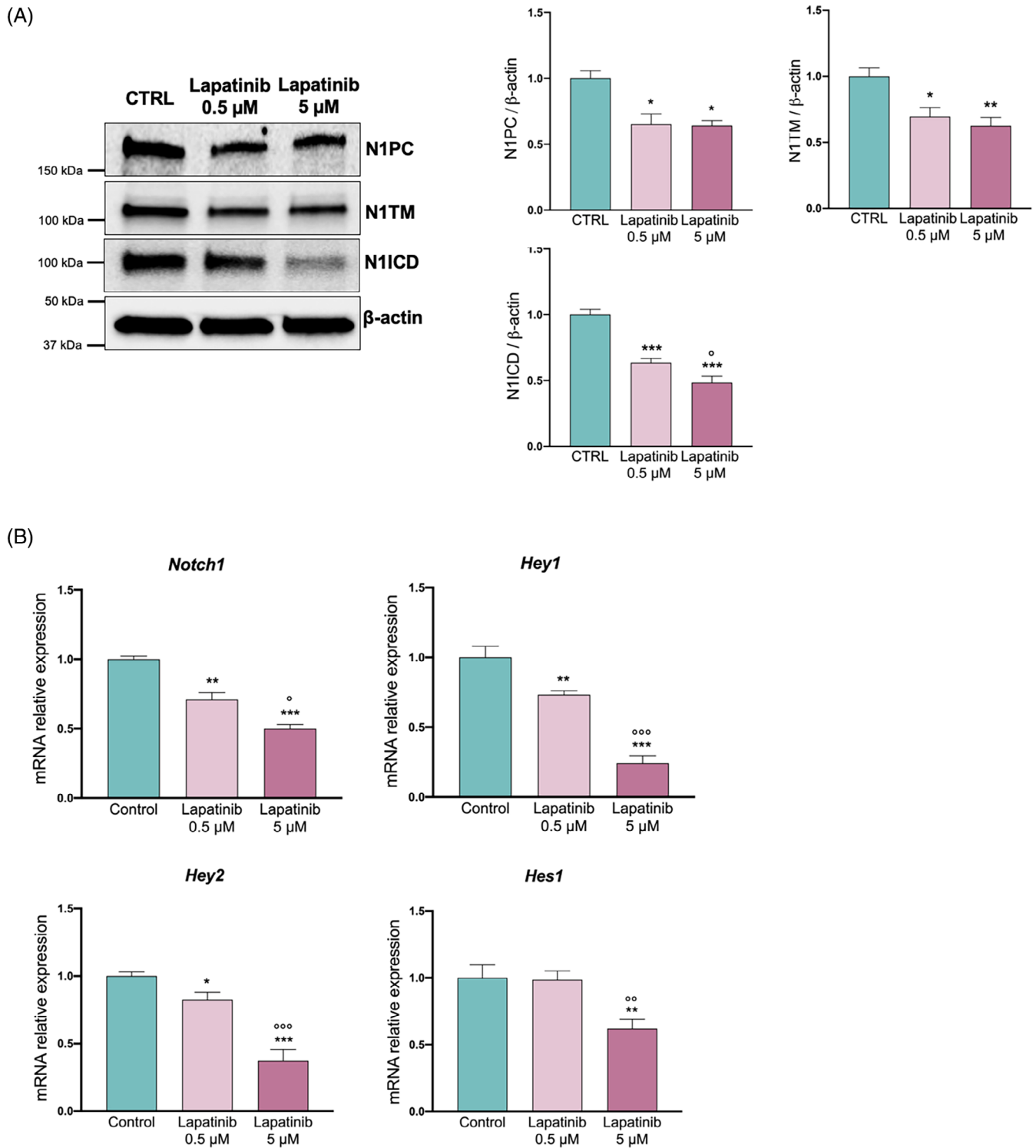
FIGURE 2 Treatment with lapatinib inhibits Notch1 activation. H9c2 cells were treated with DMSO (CTRL) or lapatinib 0.5 and 5 μM for 24 h and the following analyses were performed: (A) (left) Western blot analysis of the protein levels of precursor (N1PC), transmembrane (N1TM) and active form of Notch1 (N1ICD). β-Actin was used as loading control; (right) Densitometric analysis of Western blots showing protein levels after the treatment with lapatinib normalized to untreated control levels, after signal comparison to β-Actin. Results are expressed as mean ± SEM of three independent experiments. *$p < 0.05$; **$p < 0.01$, ***$p < 0.001$ (pairwise comparison between CTRL and treatments);°$p < 0.05$ (pairwise comparison between lapatinib 0.5 and 5 μM). (B) qRT-PCR analyses to determine *Notch1*, *Hey1*, *Hey2*, and *Hes1* mRNA levels. Relative changes in mRNA expression levels were calculated according to the $2^{-\Delta\Delta Ct}$ method using *Rpl13A* as reference gene. Results are expressed as mean ± SEM of three independent experiments. *$p < 0.05$; **$p < 0.01$; and ***$p < 0.001$ (pairwise comparison between CTRL and treatments);°$p < 0.05$;°°$p < 0.01$; and°°°$p < 0.001$ (pairwise comparison between lapatinib 0.5 and 5 μM).
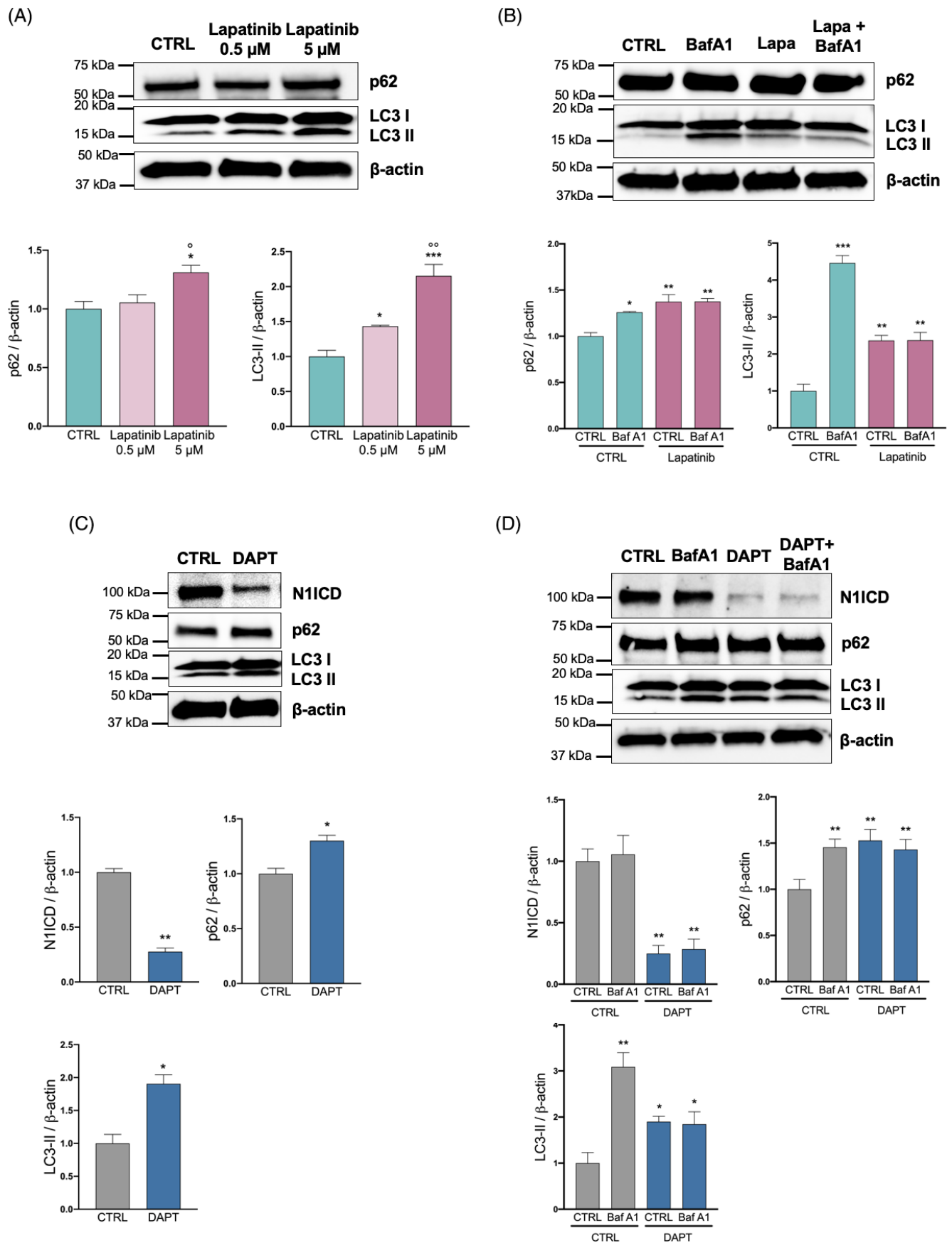
FIGURE 3 Legend on next page.

negative impact of lapatinib on cell proliferation, we transfected H9c2 cells with N1ICD or an empty vector. Re-expression of N1ICD counteracted the reduction of cell proliferation caused by lapatinib after 72 h of treatment (Figure 6A).

As expected, and consistent with data shown in Figure 5B, overexpression of N1ICD did not affect apoptosis or senescence, either in the presence or absence of lapatinib (Supplementary Figures S5 and S6). Treatment with lapatinib 5 μM for 24 and 48 h, either with or without N1ICD overexpression, did not significantly modulate the levels of caspase-3 full-length (FL) and cleaved forms, and Bax or Bcl-2 proteins (Supplementary Figure S5B). Similarly, no differences were observed in the number of SA-β-gal-positive H9c2 cells after the treatment with 5 μM lapatinib for 48 or 72 h, with or without the overexpression of N1ICD (Supplementary Figure S6).

We further investigated the mechanism by which ectopic N1ICD expression counteracts the effects of lapatinib on cell proliferation by analyzing the expression of the nuclear protein Ki67, which is present exclusively in proliferating cells.[46] Treatment with lapatinib 5 μM for 24, 48, and 72 h reduced the percentage of Ki67 positive (Ki67+) cells and overexpression of N1ICD prevented this reduction (Figure 6B). Consistently, treatment with lapatinib 5 μM for 48 and 72 h increased cell population in G0/G1—phase and reduced percentage of cells in S/G2/M phase. H9c2 cells overexpressing N1ICD exhibited a trend towards a decreased percentage of the cell population in G0/G1 and an increased percentage in S/G2/M (Supplementary Figure S7). These results indicate that active Notch1 counteracts lapatinib-induced reduction of cell proliferation by promoting cell cycle progression.

3.6 | ErbB2 controls Notch1 activation in primary mouse cardiomyocytes and in vivo

To confirm the data obtained with H9c2 cells, primary mouse neonatal cardiomyocytes were treated with NRG-1 to activate ErbB2 signaling, with or without the γ-secretase inhibitor MK-0752 (MK) at a concentration of 5 μM. Proliferation of cardiomyocytes was assessed by counting the number of Ki67/troponin T double positive cells. As shown in Figure 7A, exogenous NRG-1 significantly increased cell proliferation and this effect was antagonized by inhibition of γ-secretase and, thereby, Notch1 activation. Thus, Notch1 mediates ErbB2-dependent proliferation in primary mouse cardiomyocytes like it does in the H9c2 cell line. Furthermore, the hearts of ErbB2^{tg} mice were characterized by increased N1ICD protein levels as compared with wild-type littermates, while N1TM was not modulated (Figure 7B).

Next, we performed microarray analysis on the RNA extracted from the hearts of wild-type and ErbB2^{tg} mice. In total, we identified 2494 DEGs. We selected a panel of 184 genes related to Notch signaling based on Mouse Molecular Signatures Database (MSigDB, https://www.gsea-msigdb.org/gsea/msigdb/index.jsp) and found that 100 of them were expressed and detected in our array, highlighting the importance of Notch in the heart. Among the 100 genes related to Notch signaling, 52 were differentially expressed between ErbB2^{tg} and wild-type

---

FIGURE 3 Treatment with lapatinib or with DAPT blocks autophagic flux. (A) H9c2 cells were treated with DMSO (CTRL) or lapatinib (Lapa) 0.5 and 5 μM for 24 h and were performed Western blot analysis of the protein levels of LC3-I/II and p62. β-Actin was used as loading control. Densitometric analysis of Western blots showing protein levels after the treatment with lapatinib normalized to untreated control levels, after signal comparison to β-Actin. Results are expressed as mean ± SEM of three independent experiments. *$p < 0.05$; ***$p < 0.001$ (pairwise comparison between CTRL and treatments);°$p < 0.05$;°°$p < 0.01$ (pairwise comparison between lapatinib 0.5 and 5 μM). (B) H9c2 cells were treated with lapatinib 5 μM for 24 h in the presence or absence of bafilomycin A1 (BafA1) 100 nM during the last 4 h of the treatment and, then, Western blot analysis was performed to determine LC3-I/II and p62 protein levels. β-Actin was used as loading control. Densitometric analysis of Western blots showing protein levels after the treatments normalized to untreated control levels, after signal comparison to β-Actin. Results are expressed as mean ± SEM of three independent experiments. *$p < 0.05$; **$p < 0.01$; ***$p < 0.001$. (C) H9c2 cells were treated with DAPT 5 μM for 24 h and Western blot analysis was performed to determine N1ICD (active Notch1), p62, and LC3-I/II protein levels. β-Actin was used as loading control. Densitometric analysis of Western blots showing protein levels after the treatment with DAPT normalized to untreated control levels, after signal comparison to β-Actin. Results are expressed as the mean ± SEM of three independent experiments. *$p < 0.05$; **$p < 0.01$. (D) H9c2 were treated with DAPT 5 μM for 24 h in the presence or absence of bafilomycin A1 (BafA1) 100 nM during the last 4 h of the treatment and Western blot analysis was performed to determine N1ICD, LC3I/II, and p62 protein levels. β-Actin was used as loading control. Densitometric analysis of Western blots showing protein levels after the treatments normalized to untreated control levels, after signal comparison to β-Actin. Results are expressed as mean ± SEM of three independent experiments. *$p < 0.05$; **$p < 0.01$.
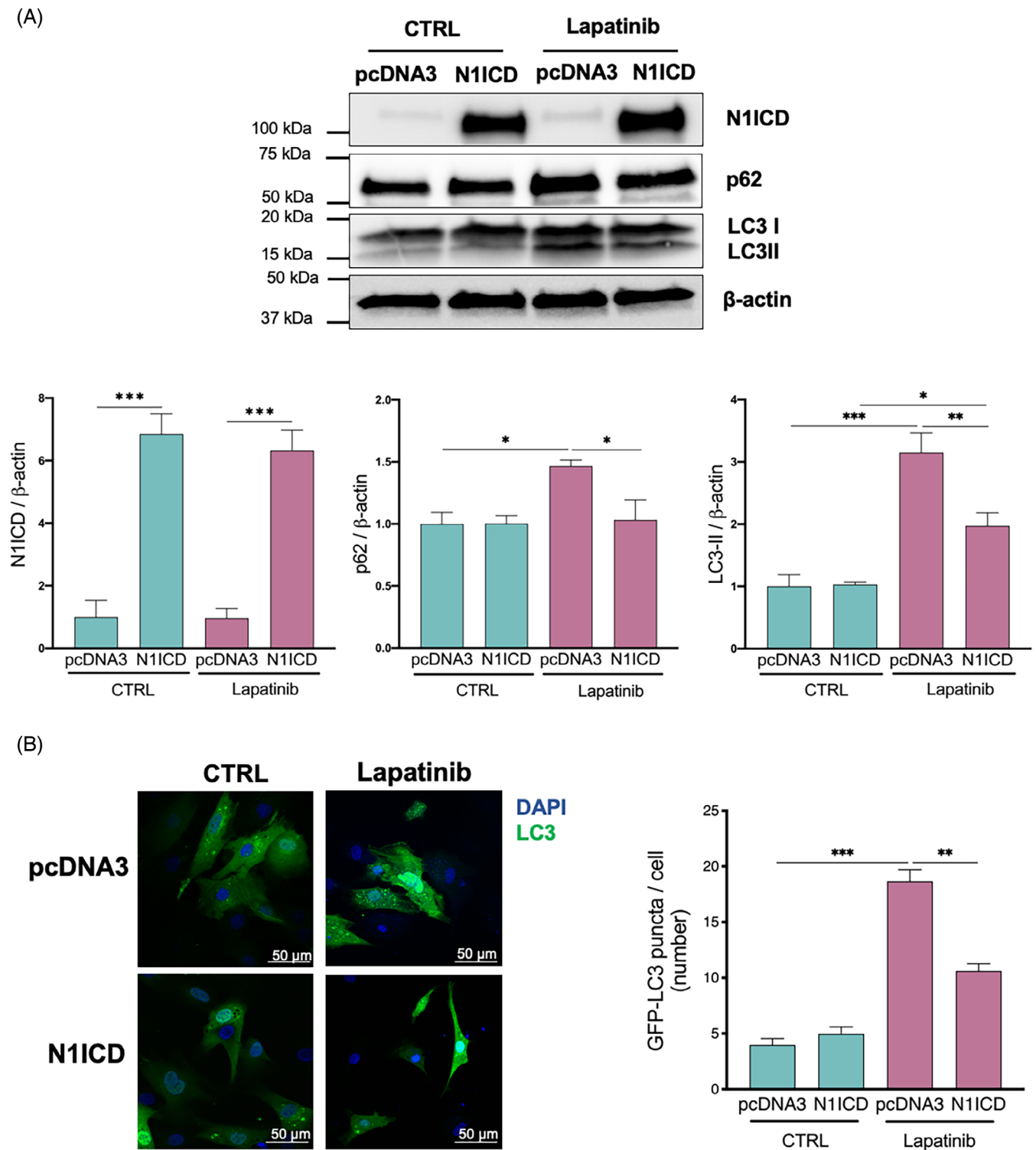
(A)

(B)

FIGURE 4 Overexpression of Notch1 rescues autophagic flux impaired by lapatinib treatment. (A) H9c2 cells were transfected with a plasmid encoding the active form of Notch1 (N1ICD) or with empty vector as control (pcDNA3) in the presence or absence of lapatinib 5 μM for 24 h and the following analyses were performed: (Top) Western blot analysis of the levels of Notch1 intracellular domain (N1ICD), p62 and LC3-I/II. β-Actin was used as loading control. (Bottom) Densitometric analysis of Western blots showing protein levels after the treatments normalized to untreated control levels, after signal comparison to β-Actin. Results are expressed as the mean $\pm$ SEM of three independent experiments. * $p < 0.05$; ** $p < 0.01$; *** $p < 0.001$. (B) Detection of autophagy activity through GFP-LC3 puncta (60× magnification). The graph shows the mean number of GFP-LC3 dots per cell counted in three visual fields of three independent experiments. Results are expressed as the mean $\pm$ SEM. ** $p < 0.01$; *** $p < 0.001$.
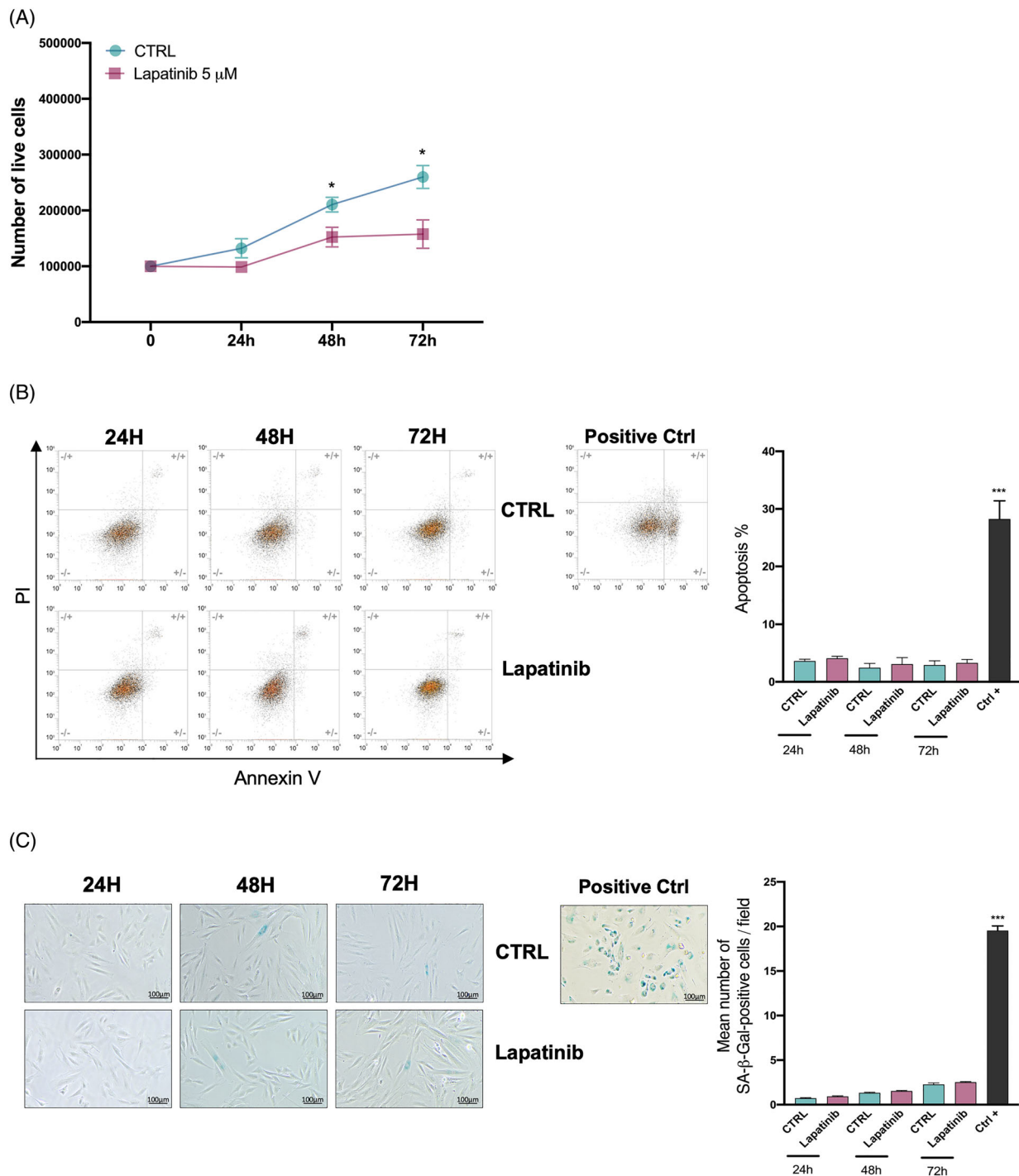
FIGURE 5 Treatment with lapatinib reduces cell proliferation but does not induce apoptosis or senescence in H9c2 cells. (A) H9c2 cells were plated in 6-wells plates and treated with DMSO (CTRL) or lapatinib 5 μM for 24, 48, and 72 h and cell were counted. Results are expressed as a mean ± SEM of three independent experiments. *$p < 0.05$. (B) H9c2 cells were treated with DMSO (CTRL) and lapatinib 5 μM for 24, 48, and 72 h and then stained with Annexin V and PI for flow cytometric analysis of apoptosis. (Left) Representative flow cytometry plots are shown for each treatment (+/+ Annexin V-positive PI-positive; +/− Annexin V-positive PI-negative; −/+ Annexin V-negative PI-positive; −/− Annexin V-negative PI-negative). As a technical positive control, H9c2 cells were treated as reported in the Methods section. (Right) Graph shows percentage of apoptotic cells (ratio of Annexin V-positive cells/total cells). Data are expressed as mean ± SEM of three independent experiments. *** $p < 0.001$ (different from any condition). C) H9c2 cells were treated with DMSO (CTRL) and lapatinib 5 μM for 24, 48, and 72 h and then stained for senescence associated β-galactosidase (SA-β-gal) for senescence analysis. (Left) Representative images of SA-β-gal staining and (right) quantification of the blue-stained cells. As a technical positive control, HUVECs were treated as reported in the Methods section. Results are expressed as the mean of SA-β-gal-positive cells counted in 5 visual fields of three independent experiments. *** $p < 0.001$ (different from any condition).
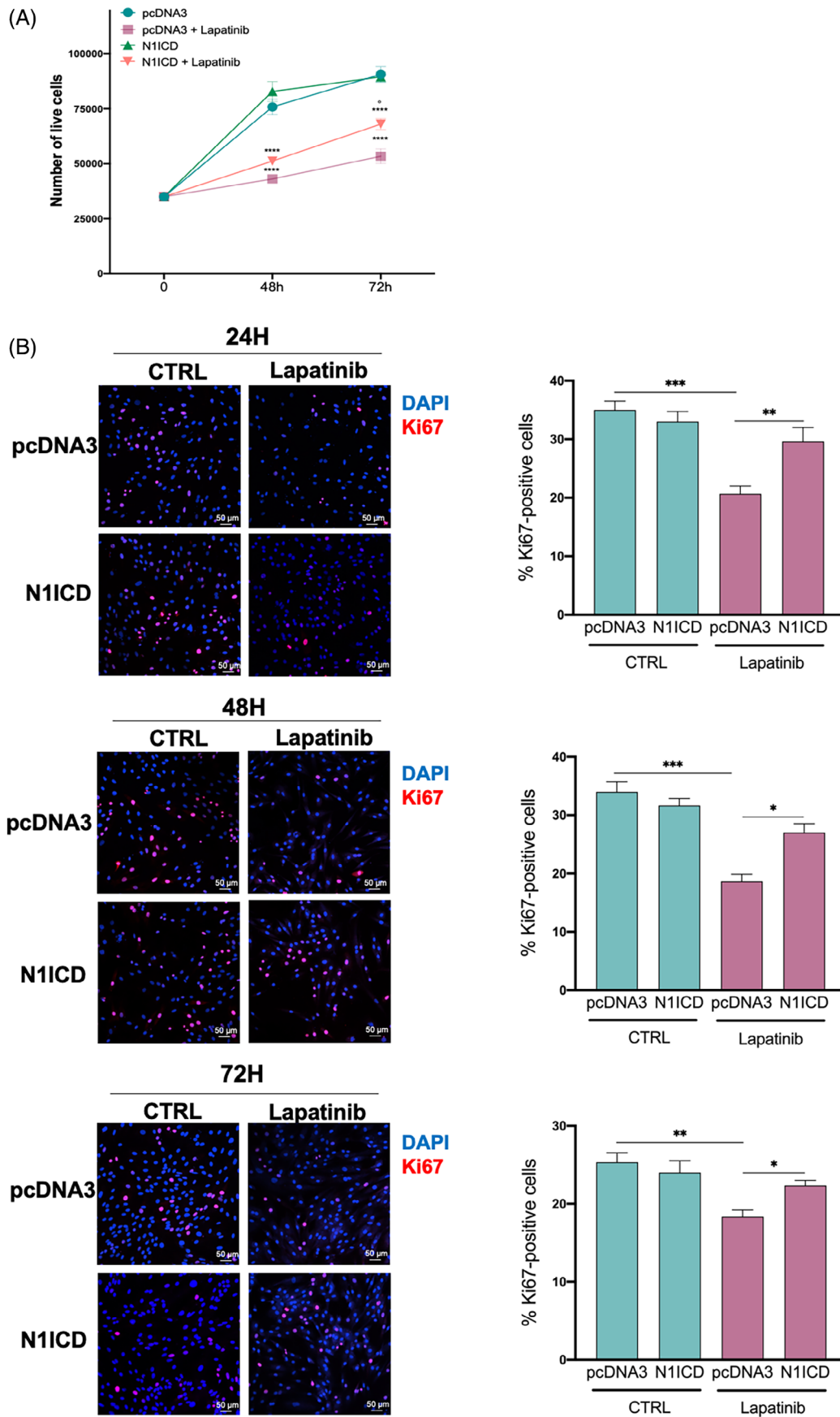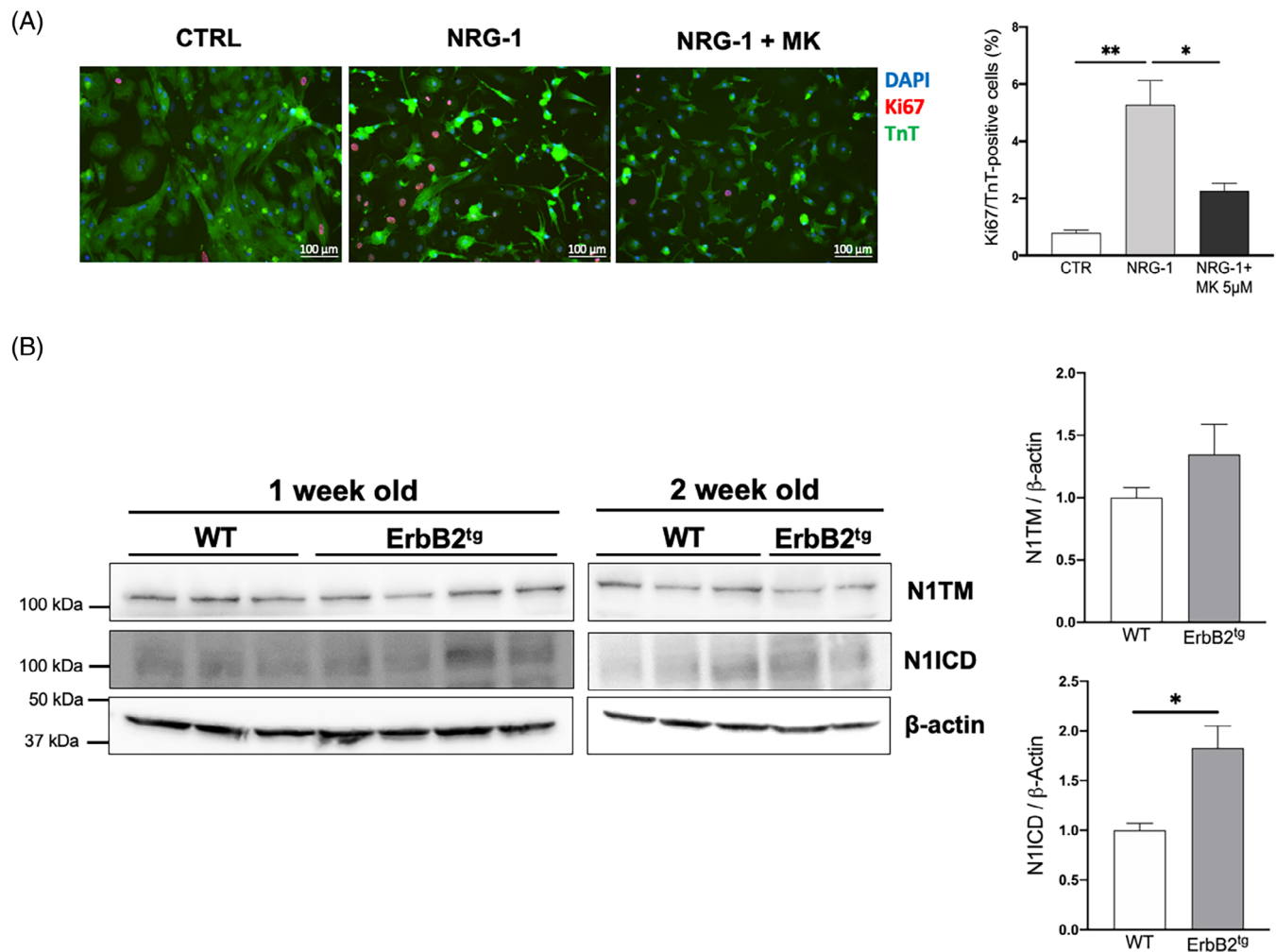
FIGURE 6 Legend on next page.

(A)

(B)

FIGURE 7 ErbB2 controls Notch1 activation in primary mouse cardiomyocytes and in vivo. (A) Mouse neonatal cardiomyocytes were treated for 72 h with 100 nM neuregulin-1 (NRG-1), in the presence or absence of a Notch inhibitor (5 μM MK0752) and proliferation was assessed by co-staining for Ki67 and cardiac troponin T (TnT). (Left) Representative images (20× magnification) of immunofluorescence staining against Ki67 (red) and cardiac troponin T (green). Nuclei were counterstained with DAPI (blue). (Right) Ki67/TnT double positive cells were counted, and percentage of Ki67/TnT-positive cells was calculated and plotted as mean ± SEM from three independent experiments, *$p < 0.05$; **$p < 0.01$. Tukey's post-hoc test. (B) (Left) Hearts of 1 and 2 week of age Her-2/neuT transgenic mice (Tg) overexpressing ErbB2 specifically in cardiomyocytes were lysed and pooled Western blot analysis of the levels of Notch1 transmembrane (N1TM) and cleaved Notch1 (N1ICD) was performed. β-Actin antibody was used to ensure equal loading. (Right) Densitometric analysis of Western blots showing protein levels after the treatments normalized to untreated control levels, after signal comparison to β-Actin. Results are expressed as the mean ± SEM. *$p < 0.05$.

mice, confirming ErbB2-mediated regulation of Notch in the heart (Supplementary Figure S8 and Tables 1 and 2). Among the receptors and ligands of Notch, we found that

Jagged1 and *Jagged2* were upregulated, while *Notch3* was downregulated in ErbB2^{tg} vs wild-type mice. Other Notch pathway components expressed in cardiomyocytes,

FIGURE 6 Overexpression of Notch1 counteracts the lapatinib-mediated reduction of cell proliferation and cell cycle progression. (A) H9c2 were plated in 12-wells plates, transfected with the plasmid containing the sequence for the active form of Notch1 (N1ICD), or pcDNA3 (empty vector), then treated with lapatinib 5 μM for 48 and 72 h, and cells were counted. Results are expressed as mean ± SEM of three independent experiments. **** $p < 0.0001$; °$p < 0.05$ (pairwise comparison between plus and minus N1ICD). (B) Immunofluorescence staining of Ki67 (red) in H9c2 transfected with active Notch1 (N1ICD) or the empty vector (pcDNA3) in presence or absence of lapatinib 5 μM for 24, 48, and 72 h. DAPI (blue) highlights cell nuclei. Graphs show the percentage of Ki67-positive cells counted in five visual fields of three independent experiments. Results are expressed as mean ± SEM. * $p < 0.05$; **$p < 0.01$; and ***$p < 0.001$.

TABLE 1 List of genes upregulated in the left ventricles of ErbB2^tg mice compared to wild-type littermates (FDR <0.25).

FDR	Fold change	Symbol	Definition
0	1.52	Anxa4	Annexin A4
0.0007	1.83	App	Amyloid beta (A4) precursor protein
0.0177	1.33	Arrb1	Arrestin, beta 1, transcript variant b
0.0929	1.33	Ccnc	Cyclin C
0.1022	1.13	Cdkn1b	Cyclin-dependent kinase inhibitor 1B
0.0003	1.24	Egfl7	EGF-like domain 7, transcript variant c
0.0172	1.48	Epn2	Epsin 2
0.0396	1.48	Epn2	Epsin 2
0.0176	1.45	Epn2	Epsin 2
0.0709	1.33	Fbxw7	F-box and WD-40 domain protein 7, archipelago homolog (*Drosophila*)
0.0006	1.04	Fgf10	Fibroblast growth factor 10
0.1046	1.7	Hes1	Hairy and enhancer of split 1 (*Drosophila*)
0.0679	1.13	Hey2	Hairy/enhancer-of-split related with YRPW motif 2
0.1787	1.1	Hey2	Hairy/enhancer-of-split related with YRPW motif 2
0.0474	1.46	Heyl	Hairy/enhancer-of-split related with YRPW motif-like
0.2332	1.13	Hp	Haptoglobin
0.1342	1.08	Ift172	Intraflagellar transport 172 homolog (Chlamydomonas)
0.0041	1.38	Ift88	Intraflagellar transport 88 homolog (Chlamydomonas)
0	1.36	Jag1	Jagged 1
0.1232	1.08	Jag2	Jagged 2
0	1.29	Kctd10	Potassium channel tetramerisation domain containing 10
0	2.81	Mmp14	Matrix metallopeptidase 14 (membrane-inserted)
0.0236	1.42	Notch4	Notch gene homolog 4 (*Drosophila*)
0	1.35	Notch4	Notch gene homolog 4 (*Drosophila*)
0.2203	1.28	Pofut1	Protein O-fucosyltransferase 1, transcript variant 2
0.0421	1.27	Pofut1	Protein O-fucosyltransferase 1, transcript variant 2
0.0209	1.4	Psen1	Presenilin 1
0.201	1.33	Reck	Reversion-inducing-cysteine-rich protein with kazal motifs
0.0264	1	Rfng	RFNG O-fucosylpeptide 3-beta-*N*-acetylglucosaminyltransferase
0.0003	1.39	Sel1l	Sel-1 suppressor of lin-12-like (*C. elegans*), transcript variant 1
0.1763	1.14	Six1	Sine oculis-related homeobox 1 homolog (*Drosophila*)
0.002	1.5	Slc35c1	Solute carrier family 35, member C1, transcript variant 2
0	1.53	Sox9	SRY-box containing gene 9
0.1371	1.31	Stat3	Signal transducer and activator of transcription 3, transcript variant 1
0.0001	2.07	Tgfb2	Transforming growth factor, beta 2
0.0188	1.33	Tgfbr2	Transforming growth factor, beta receptor II, transcript variant 1
0	2.55	Tmem100	Transmembrane protein 100
0.0433	1.48	Traf7	Tnf receptor-associated factor 7
0.0055	1.15	Zfp423	Zinc finger protein 423

Notch1, *4* and *Dll1*, *Dll4*, were not differently expressed in ErbB2^tg mice compared to wild-type littermates. Among the top 10 genes exhibiting the most pronounced differences *Mmp14*, *Tmem100*, *Tgfb2*, *App*, *Hes1*, and *Sox9* were upregulated, while *Pgam2*, *Notch3*, *Rcan2*, and *Epn1* were downregulated in ErbB2^tg mice.

TABLE 2 List of genes downregulated in the left ventricles of ErbB2^tg mice compared to wild-type littermates (FDR <0.25).

FDR	Fold change	Symbol	Definition
0.0059	−1.22	Adam17	A disintegrin and metallopeptidase domain 17
0.2056	−1.23	Akt1s1	AKT1 substrate 1 (proline-rich)
0.0589	−1.02	Aph1b	Anterior pharynx defective 1b homolog (*C. elegans*)
0.2421	−1.44	Chac1	ChaC, cation transport regulator-like 1 (*E. coli*)
0.002	−1.58	Epn1	Epsin 1
0	−1.06	Fgf10	Fibroblast growth factor 10
0.032	−1.4	Gata2	GATA binding protein 2
0.0572	−1.23	Itgb1bp1	Integrin beta 1 binding protein 1
0	−1.25	Kcna5	Potassium voltage-gated channel, shaker-related subfamily, member 5
0.0253	−1.18	Nfkbia	Nuclear factor of kappa light polypeptide gene enhancer in B-cells inhibitor, alpha
0.0187	−1.66	Notch3	Notch gene homolog 3 (*Drosophila*)
0	−2.13	Pgam2	Phosphoglycerate mutase 2
0.0254	−1.53	Ptp4a3	Protein tyrosine phosphatase 4a3
0	−1.61	Rcan2	Regulator of calcineurin 2, transcript variant 1
0.0002	−1.07	Slc35c2	Solute carrier family 35, member C2
0.003	−1.39	Spen	SPEN homolog, transcriptional regulator (*Drosophila*)
0.0185	−1.28	Synj2bp	Synaptojanin 2 binding protein
0.0021	−1.32	Synj2bp	Synaptojanin 2 binding protein
0.0023	−1.48	Timp4	Tissue inhibitor of metalloproteinase 4

4 | DISCUSSION

In this study, we explored the interplay between ErbB2 and Notch1 pathways in H9c2 cardiomyoblasts and cardiomyocytes using both pharmacological and gene overexpression methods. Our findings reveal that overexpression of ErbB2 activates Notch1, partly through a p38-dependent mechanism, while inhibition of ErbB2 with lapatinib decreases Notch1 activation. Furthermore, we observed that the inhibition of autophagic flux and proliferation induced by lapatinib in H9c2 cardiomyoblasts could be reversed by overexpressing active Notch1. Additionally, we found that the proliferation of primary neonatal mouse cardiomyocytes in response to NRG-1 was hindered when Notch1 activation was inhibited.

The Notch pathway is evolutionarily conserved, as expected for a pathway which is a major player in determining cell fate during development and in postnatal life, particularly in continuously renewing tissues where Notch controls cell stemness, differentiation, and survival. Given this role, it is not surprising that Notch is intricately intertwined with other major pathways involved in these biological processes.[47] The crosstalk between Notch and ErbB2/HER2 has been investigated thoroughly in cancer cells, where these pathways interact to modulate cell proliferation and survival.[48] In particular, in HER2 positive breast cancer, Notch1 is activated following the inhibition of ErbB2 by trastuzumab or lapatinib, contributing to resistance to both treatments.[18,49,50] One proposed mechanism for this activation is the enhanced membrane expression of the Notch ligand Jagged1.[51] However, while these studies implicate an inhibitory action of ErbB2 on Notch1, other studies have reported induction of Notch1 signaling by ErbB2 activation in breast cancer.[20]

Here we show, for the first time, that ErbB2 and Notch1 interact in H9c2 cardiomyoblasts, in which Notch1 activation is stimulated by overexpression and blunted by inhibition of ErbB2. Moreover, we provide cues of enhanced Notch1 activation in the hearts of mice with cardiac-restricted overexpression of ErbB2, showing differential expression of approximately 50 genes related to Notch signaling, including *Hes1*, *Mmp14*,[52] *Tmem100*,[53] *Tgf-β2*,[54] and *Sox9*.[55] Our data are consistent with previous studies showing that Notch1 is involved in the response to physiological recruitment of ErbB2 by NRG-1. Specifically, in zebrafish, Notch signaling is activated by ErbB2 in cardiomyocytes to direct ventricular chamber morphogenesis and, in turn, Notch signaling cell-autonomously inhibits ErbB2 signaling.[56] In addition, in mice, Notch1 regulates cardiac morphogenesis through the EphrinB2- and Hand2-mediated expression of NRG-1.[56,57]

Consistently with previous studies in human fibroblasts showing that Notch1 signaling is activated by oncogenic Ras through a p38-mediated pathway[36] we found that, in H9c2, ErbB2-mediated phosphorylation is required to increase the levels of N1ICD. The mechanisms of p38-mediated activation of Notch1 remain to be determined; it may be related to increased mRNA stability[58] or to the phosphorylation of presenilin and/or nicastrin, two components of the γ-secretase complex.[59] On the other hand, Notch ligands Jagged1 and Jagged2 were found upregulated in the hearts of ErbB2^{tg} mice, hence ligand-mediated activation of Notch1 by ErbB2 is also possible. It should be mentioned that other ErbB2 downstream players such as GSK3β/β-catenin or YAP can potentially regulate Notch. Specifically, in neonatal cardiomyocytes ErbB2 inhibits GSK3β and enhances the expression level of β-catenin[60] that could activate Notch signaling.[61] Similarly, ErbB2 signaling has been shown to lead to the phosphorylation of YAP[62] which, in turn, acts upstream of Notch signaling.[63] Further studies are needed to investigate the involvement of these pathways in ErbB2-mediated Notch1 activation.

Recent studies have shown that Notch regulates autophagy in various context: cancer cells,[64] in the brain following a hypoxic–ischemic injury,[65] in the heart in the presence of oxygen and glucose deprivation-induced myocardial damage,[66] and in T cells.[42] Conversely, autophagy-mediated Notch inhibition impacts stem cell differentiation,[67] including differentiation of cardiac cells[68] and interferes with cancer cell metastasis.[69] Here, we report that Notch1 inhibition by a γ-secretase inhibitor blocks the autophagic flux in H9c2 cells similarly to lapatinib-mediated ErbB2 inhibition. In addition, we found that transient overexpression of N1ICD counteracted the stall of autophagy induced by lapatinib, indicating that, in H9c2, Notch1 modulates autophagy downstream of ErbB2. Importantly, we observed that ErbB2 inhibition also alters mitochondrial metabolism, as reflected by the increase of the mitochondria membrane potential and mitochondrial ROS production. Our findings align with previous research describing the block of autophagic flux and accumulation of damaged mitochondria following ErbB2 inhibition by trastuzumab.[11] However, while N1ICD overexpression counteracted the alteration of mitochondrial potential, it did not prevent the increase in mitochondrial ROS production, indicating that lapatinib impairs mitochondria metabolism also by other, Notch1-independent, mechanisms.

Autophagy is an evolutionarily conserved process that plays a crucial role in regulating cardiac homeostasis[70] and dysregulation of autophagy in cardiomyocytes has been implicated in the pathogenesis of a wide range of cardiac diseases, including cardiomyopathy and HF.[71,72]

Several studies suggest that tight regulation of the autophagic process in the heart is necessary because excessive activation or, conversely, blockade of autophagic flux can be detrimental. In particular, a complex relationship exists between autophagy blockade and cell survival and growth[73] and, depending on the cell context, autophagy blockade can lead to increased cell death, as damaged cellular components are not cleared away and can accumulate to toxic levels,[74] or promotes cell survival, by preventing the breakdown of critical cellular components and preserving energy reserves.[75] Similarly, autophagy blockade can lead to reduced cell growth, as the cell is unable to break down and recycle cellular components for energy or biosynthesis, but also to increased cell growth.[76] We found that blockade of the autophagic flux by ErbB2 or Notch1 inhibition was associated with decreased proliferation of H9c2 cells and that the ectopic expression of N1ICD in lapatinib-treated cells restored proliferation. These data, linking Notch to cardiac cells proliferation are consistent with those from other authors, who showed that Notch1 promotes proliferation of cardiac progenitor cells[77] and immature cardiomyocytes,[23] and induces cell cycle re-entry in quiescent cardiomyocytes.[23,78] The knowledge of the mechanisms regulating cardiac cell proliferation is crucial since adult cardiomyocytes have limited renewal capacity, inadequate for restoring the damaged heart, but that could be promoted, thus stimulating the intrinsic cardiac regenerative potential, as reported by several authors.[60,79–81]

The findings of our study expand the existing knowledge on the roles of ErbB2 and Notch1 in cardiac biology and may have translational implications when considering the cardiotoxicity of HER2-directed antitumor therapies. Although the Notch signaling pathway undergoes gradual attenuation in the postnatal heart, it can be reactivated in the adult myocardium following ischemic injury,[24,25,82] hypertrophy[83] or HF,[84] thereby reducing apoptosis and pathological hypertrophy of cardiomyocytes[25,83] as well as fibrosis.[85] Since Notch1 is central to the cardiac response to injury,[20,47] in principle, part of the cardiotoxicity of HER2 targeting drugs might lie in the inhibition of Notch1 activation, leading to impaired adaptation of the heart to various stresses.

In conclusion, our experiments show that ErbB2 is upstream of Notch1 activation in H9c2 cardiomyoblasts and in primary neonatal mouse cardiomyocytes, and that Notch1 inhibition or activation mediates at least some effects of ErbB2 inhibition or stimulation, respectively. We acknowledge that most of our findings were obtained in H9c2 cardiomyoblasts, which have similarities but also important differences with cardiomyocytes. For instance, cardiomyoblasts derived from the embryonic rat heart

have higher expression of ErbB2 than adult mature cardiomyocytes.[7] Nonetheless, primary cultures of cardiomyocytes include a certain number of noncardiomyocytes and display temporal changes in the expression of Notch receptors and Notch ligands, which make assessments such as the ones made here difficult.[23] Moreover, overexpression experiments in primary cultures are technically challenging. It is noteworthy that we collected confirmatory results with primary neonatal mouse cardiomyocytes and whole mouse hearts, suggesting that the crosstalk between ErbB2 and Notch1 does occur in vivo. Further work is needed to consolidate these findings and evaluate whether cardiac Notch1 preservation/activation may protect against the adverse effects of anti-HER2 medications in the heart.

AUTHOR CONTRIBUTIONS

FF, PA, and PR conceived and designed the study. FF, FVDS, PA, and PR wrote the manuscript. FF, FVDS, EL, GA, PSS, EB, AA, PS, AWOT, AS, KG, and GP performed experiments and analyzed data. FF, FVDS, EL, PSS, KG, GM, SP, PP, RF, ET, PA, and PR contributed to data interpretation and revised the manuscript. All authors read and approved the final version of the manuscript.

CONFLICT OF INTEREST STATEMENT

The authors have no conflicting interests to disclose in relation to this work.

ORCID

Francesca Fortini https://orcid.org/0000-0003-0807-3792
Francesco Vieceli Dalla Sega https://orcid.org/0000-0003-3445-3983
Edoardo Lazzarini https://orcid.org/0000-0001-6369-5442

REFERENCES

1. Martínez-Sáez O, Prat A. Current and future management of HER2-positive metastatic breast cancer. JCO Oncol Pract. 2021; 17:594–604.

2. Wadugu B, Kühn B. The role of neuregulin/ErbB2/ErbB4 signaling in the heart with special focus on effects on cardiomyocyte proliferation. Am J Physiol Heart Circ Physiol. 2012;302: H2139–47.

3. Grazette LP, Boecker W, Matsui T, Semigran M, Force TL, Hajjar RJ, et al. Inhibition of ErbB2 causes mitochondrial dysfunction in cardiomyocytes: implications for herceptin-induced cardiomyopathy. J Am Coll Cardiol. 2004;44:2231–8.

4. Gordon LI, Burke MA, Singh AT, Prachand S, Lieberman ED, Sun L, et al. Blockade of the erbB2 receptor induces cardiomyocyte death through mitochondrial and reactive oxygen species-dependent pathways. J Biol Chem. 2009;284:2080–7.

5. Necela BM, Axenfeld BC, Serie DJ, Kachergus JM, Perez EA, Thompson EA, et al. The antineoplastic drug, trastuzumab, dysregulates metabolism in iPSC-derived cardiomyocytes. Clin Transl Med. 2017;6:5.

6. Rohrbach S, Muller-Werdan U, Werdan K, Koch S, Gellerich NF, Holtz J. Apoptosis-modulating interaction of the neuregulin/erbB pathway with anthracyclines in regulating Bcl-xS and Bcl-xL in cardiomyocytes. J Mol Cell Cardiol. 2005; 38:485–93.

7. de Lorenzo C, Paciello R, Riccio G, Rea D, Barbieri A, Coppola C, et al. Cardiotoxic effects of the novel approved anti-ErbB2 agents and reverse cardioprotective effects of ranolazine. Onco Targets Ther. 2018;11:2241–50.

8. Timolati F, Ott D, Pentassuglia L, Giraud MN, Perriard JC, Suter TM, et al. Neuregulin-1 beta attenuates doxorubicin-induced alterations of excitation-contraction coupling and reduces oxidative stress in adult rat cardiomyocytes. J Mol Cell Cardiol. 2006;41:845–54.

9. Belmonte F, Das S, Sysa-Shah P, Sivakumaran V, Stanley B, Guo X, et al. ErbB2 overexpression upregulates antioxidant enzymes, reduces basal levels of reactive oxygen species, and protects against doxorubicin cardiotoxicity. Am J Physiol Heart Circ Physiol. 2015;309:H1271–80.

10. Jacob F, Yonis AY, Cuello F, Luther P, Schulze T, Eder A, et al. Analysis of tyrosine kinase inhibitor-mediated decline in contractile Force in rat engineered heart tissue. PLoS One. 2016; 11:e0145937.

11. Mohan N, Shen Y, Endo Y, ElZarrad MK, Wu WJ. Trastuzumab, but not Pertuzumab, dysregulates HER2 signaling to mediate inhibition of autophagy and increase in reactive oxygen species production in human cardiomyocytes. Mol Cancer Ther. 2016;15:1321–31.

12. Slamon DJ, Clark GM, Wong SG, Levin WJ, Ullrich A, McGuire WL. Human breast cancer: correlation of relapse and survival with amplification of the HER-2/neu oncogene. Science. 1987;235:177–82.

13. Nemeth BT, Varga ZV, Wu WJ, Pacher P. Trastuzumab cardiotoxicity: from clinical trials to experimental studies. Br J Pharmacol. 2017;174:3727–48.

14. Denegri A, Moccetti T, Moccetti M, Spallarossa P, Brunelli C, Ameri P. Cardiac toxicity of trastuzumab in elderly patients with breast cancer. J Geriatr Cardiol. 2016;13:355–63.

15. de Keulenaer GW, Doggen K, Lemmens K. The vulnerability of the heart as a pluricellular paracrine organ: lessons from unexpected triggers of heart failure in targeted ErbB2 anticancer therapy. Circ Res. 2010;106:35–46.

16. Kitani T, Ong SG, Lam CK, Rhee JW, Zhang JZ, Oikonomopoulos A, et al. Human-induced pluripotent stem cell model of Trastuzumab-induced cardiac dysfunction in patients with breast cancer. Circulation. 2019;139:2451–65.

17. Lindsay J, Jiao X, Sakamaki T, Casimiro MC, Shirley LA, Tran TH, et al. ErbB2 induces Notch1 activity and function in breast cancer cells. Clin Transl Sci. 2008;1:107–15.

18. Osipo C, Patel P, Rizzo P, Clementz AG, Hao L, Golde TE, et al. ErbB-2 inhibition activates Notch-1 and sensitizes breast cancer cells to a gamma-secretase inhibitor. Oncogene. 2008; 27:5019–32.

19. Marracino L, Fortini F, Bouhamida E, Camponogara F, Severi P, Mazzoni E, et al. Adding a "notch" to cardiovascular disease therapeutics: a MicroRNA-based approach. Front Cell Dev Biol. 2021;9:695114.

20. Ferrari R, Rizzo P. The notch pathway: a novel target for myocardial remodelling therapy? Eur Heart J. 2014;35:2140–5.

21. Zhou XL, Wu X, Xu QR, Zhu RR, Xu H, Li YY, et al. Notch1 provides myocardial protection by improving mitochondrial quality control. J Cell Physiol. 2019;234:11835–41.

22. Pei H, Song X, Peng C, Tan Y, Li Y, Li X, et al. TNF-α inhibitor protects against myocardial ischemia/reperfusion injury via Notch1-mediated suppression of oxidative/nitrative stress. Free Radic Biol Med. 2015;82:114–21.

23. Collesi C, Zentilin L, Sinagra G, Giacca M. Notch1 signaling stimulates proliferation of immature cardiomyocytes. J Cell Biol. 2008;183:117–28.

24. Gude NA, Emmanuel G, Wu W, Cottage CT, Fischer K, Quijada P, et al. Activation of notch-mediated protective signaling in the myocardium. Circ Res. 2008;102:1025–35.

25. Kratsios P, Catela C, Salimova E, Huth M, Berno V, Rosenthal N, et al. Distinct roles for cell-autonomous notch signaling in cardiomyocytes of the embryonic and adult heart. Circ Res. 2010;106:559–72.

26. Zhou XL, Wan L, Xu QR, Zhao Y, Liu JC. Notch signaling activation contributes to cardioprotection provided by ischemic preconditioning and postconditioning. J Transl Med. 2013; 11:251.

27. Yu B, Song B. Notch 1 signalling inhibits cardiomyocyte apoptosis in ischaemic postconditioning. Heart Lung Circ. 2014;23: 152–8.

28. Nistri S, Sassoli C, Bani D. Notch signaling in ischemic damage and fibrosis: evidence and clues from the heart. Front Pharmacol. 2017;8:187.

29. Fedele C, Riccio G, Malara AE, D'Alessio G, de Lorenzo C. Mechanisms of cardiotoxicity associated with ErbB2 inhibitors. Breast Cancer Res Treat. 2012;134:595–602.

30. Burris HA, Taylor CW, Jones SF, Koch KM, Versola MJ, Arya N, et al. A phase I and pharmacokinetic study of oral lapatinib administered once or twice daily in patients with solid malignancies. Clin Cancer Res. 2009;15:6702–8.

31. Vieceli Dalla Sega VD, Fortini F, Licastro D, Monego SD, Degasperi M, Ascierto A, et al. Serum from COVID-19 patients promotes endothelial cell dysfunction through protease-activated receptor 2. Inflamm Res. 2024;73:117–30.

32. Sega VD, Mastrocola R, Aquila G, Fortini F, Fornelli C, Zotta A, et al. KRIT1 deficiency promotes aortic endothelial dysfunction. Int J Mol Sci. 2019;20:4930.

33. Sega VD, Palumbo D, Fortini F, D'Agostino Y, Cimaglia P, Marracino L, et al. Transcriptomic profiling of calcified aortic valves in clonal hematopoiesis of indeterminate potential carriers. Sci Rep. 2022;12:20400.

34. Wojtala A, Bonora M, Malinska D, Pinton P, Duszynski J, Wieckowski MR. Methods to monitor ROS production by fluorescence microscopy and fluorometry. Methods Enzymol. 2014; 542:243–62.

35. Sysa-Shah P, Xu Y, Guo X, Belmonte F, Kang B, Bedja D, et al. Cardiac-specific over-expression of epidermal growth factor receptor 2 (ErbB2) induces pro-survival pathways and hypertrophic cardiomyopathy in mice. PLoS One. 2012;7:e42805.

36. Weijzen S, Rizzo P, Braid M, Vaishnav R, Jonkheer SM, Zlobin A, et al. Activation of Notch-1 signaling maintains the neoplastic phenotype in human Ras-transformed cells. Nat Med. 2002;8:979–86.

37. Vaishnav D, Jambal P, Reusch JE, Pugazhenthi S. SP600125, an inhibitor of c-jun N-terminal kinase, activates CREB by a p38 MAPK-mediated pathway. Biochem Biophys Res Commun. 2003;307:855–60.

38. Leemasawat K, Phrommintikul A, Chattipakorn SC, Chattipakorn N. Mechanisms and potential interventions associated with the cardiotoxicity of ErbB2-targeted drugs: insights from in vitro, in vivo, and clinical studies in breast cancer patients. Cell Mol Life Sci. 2020;77:1571–89.

39. Morano M, Angotti C, Tullio F, Gambarotta G, Penna C, Pagliaro P, et al. Myocardial ischemia/reperfusion upregulates the transcription of the Neuregulin1 receptor ErbB3, but only postconditioning preserves protein translation: role in oxidative stress. Int J Cardiol. 2017;233:73–9.

40. Curry CL, Reed LL, Nickoloff BJ, Miele L, Foreman KE. Notch-independent regulation of Hes-1 expression by c-Jun N-terminal kinase signaling in human endothelial cells. Lab Investig. 2006;86:842–52.

41. Mohan N, Jiang J, Wu WJ. Implications of autophagy and oxidative stress in Trastuzumab-mediated cardiac toxicities. Austin Pharmacol Pharm. 2017;2:1005.

42. Marcel N, Sarin A. Notch1 regulated autophagy controls survival and suppressor activity of activated murine T-regulatory cells. elife. 2016;5:e14023.

43. Yoshii SR, Mizushima N. Monitoring and measuring autophagy. Int J Mol Sci. 2017;18:1865.

44. Klionsky DJ, Abdalla FC, Abeliovich H, Abraham RT, Acevedo-Arozena A, Adeli K, et al. Guidelines for the use and interpretation of assays for monitoring autophagy. Autophagy. 2012;8:445–544.

45. Morciano G, Patergnani S, Pedriali G, Cimaglia P, Mikus E, Calvi S, et al. Impairment of mitophagy and autophagy accompanies calcific aortic valve stenosis favouring cell death and the severity of disease. Cardiovasc Res. 2022;118:2548–59.

46. Gerdes J, Lemke H, Baisch H, Wacker HH, Schwab U, Stein H. Cell cycle analysis of a cell proliferation-associated human nuclear antigen defined by the monoclonal antibody Ki-67. J Immunol. 1984;133:1710–5.

47. Aquila G, Kostina A, Sega VD, Shlyakhto E, Kostareva A, Marracino L, et al. The notch pathway: a novel therapeutic target for cardiovascular diseases? Expert Opin Ther Targets. 2019;23:695–710.

48. Zhang K, Wong P, Salvaggio C, Salhi A, Osman I, Bedogni B. Synchronized targeting of notch and ERBB signaling suppresses melanoma tumor growth through inhibition of Notch1 and ERBB3. J Invest Dermatol. 2016;136:464–72.

49. Pandya K, Meeke K, Clementz AG, Rogowski A, Roberts J, Miele L, et al. Targeting both notch and ErbB-2 signalling pathways is required for prevention of ErbB-2-positive breast tumour recurrence. Br J Cancer. 2011;105:796–806.

50. Baker AT, Zlobin A, Osipo C. Notch-EGFR/HER2 bidirectional crosstalk in breast cancer. Front Oncol. 2014;4:360.

51. Shah D, Wyatt D, Baker AT, Simms P, Peiffer DS, Fernandez M, et al. Inhibition of HER2 increases JAGGED1-dependent breast cancer stem cells: role for membrane JAGGED1. Clin Cancer Res. 2018;24:4566–78.

52. Chang JH, Huang YH, Cunningham CM, Han KY, Chang M, Seiki M, et al. Matrix metalloproteinase 14 modulates signal transduction and angiogenesis in the cornea. Surv Ophthalmol. 2016;61:478–97.

53. Moon EH, Kim YH, Vu PN, Yoo H, Hong K, Lee YJ, et al. TMEM100 is a key factor for specification of lymphatic endothelial progenitors. Angiogenesis. 2020;23:339–55.

54. Klüppel M, Wrana JL. Turning it up a Notch: cross-talk between TGF beta and Notch signaling. BioEssays. 2005;27: 115–8.

55. Kohn A, Rutkowski TP, Liu Z, Mirando AJ, Zuscik MJ, O'Keefe RJ, et al. Notch signaling controls chondrocyte hypertrophy via indirect regulation of Sox9. Bone Res. 2015; 3:15021.

56. Han P, Bloomekatz J, Ren J, Zhang R, Grinstein JD, Zhao L, et al. Coordinating cardiomyocyte interactions to direct ventricular chamber morphogenesis. Nature. 2016;534:700–4.

57. VanDusen NJ, Casanovas J, Vincentz JW, Firulli BA, Osterwalder M, Lopez-Rios J, et al. Hand2 is an essential regulator for two notch-dependent functions within the embryonic endocardium. Cell Rep. 2014;9:2071–83.

58. Frank SB, Berger PL, Ljungman M, Miranti CK. Human prostate luminal cell differentiation requires NOTCH3 induction by p38-MAPK and MYC. J Cell Sci. 2017;130:1952–64.

59. Kuo LH, Hu MK, Hsu WM, Tung YT, Wang BJ, Tsai WW, et al. Tumor necrosis factor-alpha-elicited stimulation of gamma-secretase is mediated by c-Jun N-terminal kinase-dependent phosphorylation of presenilin and nicastrin. Mol Biol Cell. 2008;19:4201–12.

60. D'Uva G, Aharonov A, Lauriola M, Kain D, Yahalom-Ronen Y, Carvalho S, et al. ERBB2 triggers mammalian heart regeneration by promoting cardiomyocyte dedifferentiation and proliferation. Nat Cell Biol. 2015;17:627–38.

61. Zheng L, Conner SD. Glycogen synthase kinase 3β inhibition enhances Notch1 recycling. Mol Biol Cell. 2018;29:389–95.

62. Aharonov A, Shakked A, Umansky KB, Savidor A, Genzelinakh A, Kain D, et al. ERBB2 drives YAP activation and EMT-like processes during cardiac regeneration. Nat Cell Biol. 2020;22:1346–56.

63. Engel-Pizcueta C, Pujades C. Interplay between notch and YAP/TAZ pathways in the regulation of cell fate during embryo development. Front Cell Dev Biol. 2021;9:711531.

64. Das A, Narayanam MK, Paul S, Mukhnerjee P, Ghosh S, Dastidar DG, et al. A novel triazole, NMK-T-057, induces autophagic cell death in breast cancer cells by inhibiting γ-secretase-mediated activation of notch signaling. J Biol Chem. 2019;294:6733–50.

65. Li K, Lu M, Cui M, Wang X, Zheng Y. The notch pathway regulates autophagy after hypoxic-ischemic injury and affects synaptic plasticity. Brain Struct Funct. 2023;228:985–96.

66. Kong LY, Xi Z, Ma WT, Yang FY, Niu LD, Shi JH. Effects of notch signal on the expressions of HIF-α and autophagy-related genes Beclin1, LC3I, LC3II in oxygen-glucose deprivation induced myocardial cell injury. Zhongguo Ying Yong Sheng Li Xue Za Zhi. 2019;35:165–8.

67. Wu X, Fleming A, Ricketts T, Pavel M, Virgin H, Menzies FM, et al. Autophagy regulates notch degradation and modulates stem cell development and neurogenesis. Nat Commun. 2016; 7:10533.

68. Jia Z, Wang J, Wang W, Tian Y, XiangWei W, Chen P, et al. Autophagy eliminates cytoplasmic β-catenin and NICD to promote the cardiac differentiation of P19CL6 cells. Cell Signal. 2014;26:2299–305.

69. Zada S, Hwang JS, Lai TH, Pham TM, Ahmed M, Elashkar O, et al. Autophagy-mediated degradation of NOTCH1 intracellular domain controls the epithelial to mesenchymal transition and cancer metastasis. Cell Biosci. 2022;12:17.

70. Kaludercic N, Maiuri MC, Kaushik S, Fernández Á, de Bruijn J, Castoldi F, et al. Comprehensive autophagy evaluation in cardiac disease models. Cardiovasc Res. 2020;116: 483–504.

71. Willis MS, Patterson C. Proteotoxicity and cardiac dysfunction—Alzheimer's disease of the heart? N Engl J Med. 2013;368:455–64.

72. Ikeda S, Zablocki D, Sadoshima J. The role of autophagy in death of cardiomyocytes. J Mol Cell Cardiol. 2022;165:1–8.

73. Mathiassen SG, de Zio D, Cecconi F. Autophagy and the cell cycle: a complex landscape. Front Oncol. 2017;7:51.

74. Bonora M, Giorgi C, Pinton P. Molecular mechanisms and consequences of mitochondrial permeability transition. Nat Rev Mol Cell Biol. 2022;23:266–85.

75. Denton D, Xu T, Kumar S. Autophagy as a pro-death pathway. Immunol Cell Biol. 2015;93:35–42.

76. Neufeld TP. Autophagy and cell growth—the yin and yang of nutrient responses. J Cell Sci. 2012;125:2359–68.

77. Urbanek K, Cabral-da-Silva MC, Ide-Iwata N, Maestroni S, Delucchi F, Zheng H, et al. Inhibition of notch1-dependent cardiomyogenesis leads to a dilated myopathy in the neonatal heart. Circ Res. 2010;107:429–41.

78. Campa VM, Gutiérrez-Lanza R, Cerignoli F, Díaz-Trelles R, Nelson B, Tsuji T, et al. Notch activates cell cycle reentry and progression in quiescent cardiomyocytes. J Cell Biol. 2008;183: 129–41.

79. Bongiovanni C, Sacchi F, da Pra S, Pantano E, Miano C, Morelli MB, et al. Reawakening the intrinsic cardiac regenerative potential: molecular strategies to boost dedifferentiation and proliferation of endogenous cardiomyocytes. Front Cardiovasc Med. 2021;8:750604.

80. Pianca N, Sacchi F, Umansky KB, Chirivì M, Iommarini L, Da Pra S, et al. Glucocorticoid receptor antagonization propels endogenous cardiomyocyte proliferation and cardiac regeneration. Nat Cardiovasc Res. 2022;1:617–33.

81. Ahmed MS, Nguyen NUN, Nakada Y, Hsu C-C, Farag A, Lam NT, et al. Identification of FDA-approved drugs that

induce heart regeneration in mammals. Nat Cardiovasc Res. 2024;3(3):372–88.

82. Kore RA, Jenkins SV, Jamshidi-Parsian A, Tackett AJ, Griffin RJ, Ayyadevara S, et al. Proteomic analysis of transcription factors involved in the alteration of ischemic mouse heart as modulated by MSC exosomes. Biochem Biophys Rep. 2023; 34:101463.

83. Croquelois A, Domenighetti AA, Nemir M, Lepore M, Rosenblatt-Velin N, Radtke F, et al. Control of the adaptive response of the heart to stress via the Notch1 receptor pathway. J Exp Med. 2008;205:3173–85.

84. Øie E, Sandberg WJ, Ahmed MS, Yndestad A, Lærum OD, Attramadal H, et al. Activation of notch signaling in cardio-myocytes during post-infarction remodeling. Scand Cardiovasc J. 2010;44:359–66.

85. Zhao L, Ben-Yair R, Burns CE, Burns CG. Endocardial notch signaling promotes cardiomyocyte proliferation in the regenerating zebrafish heart through Wnt pathway antagonism. Cell Rep. 2019;26:546–554.e545.

SUPPORTING INFORMATION

Additional supporting information can be found online in the Supporting Information section at the end of this article.